*J. Fluid Mech.* (2006), *vol.* 561, *pp.* 1–42.  
doi:10.1017/S0022112006000279 Printed in the United Kingdom

# The constitutive relation for the granular flow of rough particles, and its application to the flow down an inclined plane

By V. KUMARAN

Department of Chemical Engineering, Indian Institute of Science, Bangalore 560 012, India

(Received 23 February 2004 and in revised form 7 December 2005)

A perturbation expansion of the Boltzmann equation is used to derive constitutive relations for the granular flow of rough spheres in the limit where the energy dissipation in a collision is small compared to the energy of a particle. In the collision model, the post-collisional relative normal velocity at the point of contact is $-e_n$ times the pre-collisional normal velocity, and the post-collisional relative tangential velocity at the point of contact is $-e_t$ times the pre-collisional relative tangential velocity. A perturbation expansion is employed in the limit $(1-e_n)=\varepsilon^2 \ll 1$, and $(1-e_t^2) \propto \varepsilon^2 \ll 1$, so that $e_t$ is close to $\pm 1$. In the 'rough' particle model, the normal coefficient of restitution $e_n$ is close to 1, and the tangential coefficient of restitution $e_t$ is close to 1. In the 'partially rough' particle model, the normal coefficient of restitution $e_n$ is close to 1; and the tangential coefficient of restitution $e_t$ is close to $-1$ if the angle between the relative velocity vector and the line joining the centres of the particles is greater than the 'roughness angle' (chosen to be $(\pi/4)$ in the present calculation), and is close to 1 if the angle between the relative velocity vector and the line joining the centres is less than the roughness angle. The conserved variables in this case are mass and momentum; energy is not a conserved variable in the 'adiabatic limit' considered here, when the length scale is large compared to the 'conduction length'. The results for the constitutive relations show that in the Navier–Stokes approximation, the form of the constitutive relation is identical to that for smooth particles, but the coefficient of shear viscosity for rough particles is 10 %–50 % higher than that for smooth particles. The coefficient of bulk viscosity, which is zero in the dilute limit for smooth particles, is found to be non-zero for rough and partially rough particles, owing to the transport of energy between the translational and rotational modes. In the Burnett approximation, there is an antisymmetric component in the stress tensor for rough and partially rough particles, which is not present for smooth particles.

The constitutive relations are used to analyse the 'core region' of a steady granular flow down an inclined plane, where there is a local balance between the production of energy due to the mean shear and the dissipation due to inelastic collisions. It is found that realistic results, such as the decrease in density upon increase in the angle of inclination near close packing, are obtained for the rough and partially rough particle models when the Burnett coefficients are included in the stress tensor, but realistic results are not obtained using the constitutive relations for smooth particles. This shows that the flow dynamics is sensitive to the numerical values of the viscometric coefficients, and provides an indication of the minimal model required to capture the flow dynamics.

## 1. Introduction

Much work has been done on the derivation of constitutive relations for granular materials. Kinetic theory approaches make an analogy between the motion of the particles in a granular material and the motion of molecules in a gas, and attempt to write down constitutive relations similar to those derived by the Chapman–Enskog procedure for hard sphere gases (Chapman & Cowling 1970). There have been many formulations of the balance laws and constitutive relations for smooth inelastic particles (Savage & Jeffrey 1981; Jenkins & Savage 1983; Lun *et al.* 1984; Jenkins & Richman 1985). These models typically fall into two categories, the generalized Navier–Stokes equations where the mass and momentum equations are similar to those for a simple fluid, but where the energy equation has an additional term due to the dissipation of energy in inelastic collisions (Jenkins & Savage 1983; Lun *et al.* 1984; Sela, Goldhirsch & Noskowicz 1996; Sela & Goldhirsch 1998); and the moment expansion models (Jenkins & Richman 1985; Chou & Richman 1998), where the higher moments of the velocity distribution function are incorporated in the description. There have been derivations of kinetic equations up to Burnett order starting from the Boltzmann equation using an expansion with the Knudsen number and the inelasticity of the particle collisions as the small parameters (Sela *et al.* 1996; Sela & Goldhirsch 1998). Goldhirsch (2003) concluded that hydrodynamic models have been unusually successful in describing rapid granular flows even though there is not a large scale separation between the microscopic scale (particle diameter or mean free path) and the flow scales.

There has been relatively less work on kinetic theories for rough inelastic particles, where the rotation of the particles is also incorporated. Lun & Savage (1987) developed a kinetic theory formulation for rough particles in the dense limit, where the collisional stress is large compared to the kinetic stress. Lun (1991) determined the kinetic contributions to the stresses for the dilute granular flow of slightly inelastic and slightly rough spheres, and formulated conservation laws for the density, linear and angular momenta and the linear and angular contributions to the kinetic energy. A moment expansion method was used to express the fluxes in terms of the gradients in the linear and angular velocities and temperatures. One discrepancy between the above theories and the simulations of Campbell (1989) and Walton & Braun (1986) is that the stresses in the simulations are anisotropic, whereas the theories predict isotropic stresses.

The transport properties for a dilute gas of perfectly rough elastic molecules have been calculated using the Chapman–Enskog procedure by Pidduck (1922) (see Chapman & Cowling 1970 for a description). The major conclusion of this calculation was that the equation of state for a gas of rough particles is identical to that for a gas of smooth particles, while the shear viscosity and thermal conductivity for a gas of rough particles differ by about 5 % from those for a gas of smooth particles. However, there is a significant variation in the bulk viscosity, owing to the exchange of energy between the translational and internal modes. A moment expansion method was formulated by Theodosopulu & Dahler (1974*a*, *b*) for polyatomic molecules in the dense limit, using the Boltzmann–Enskog closure approximation. In this approximation, the two-particle velocity distribution function in the BBKGY hierarchy is approximated as the product of the single-particle velocity distribution functions and the equilibrium spatial pair correlation function at contact. This approximation incorporates the increase in the pair distribution function due to excluded volume effects, but the effect of correlated collisions between particles is neglected. Theodosopulu & Dahler

(1974*a*, *b*) wrote conservation equations for the density, linear and angular momenta and the translational and rotational parts of the particle energies, and these were solved by using an expansion in the moments of the distribution function for rough particles as well as for ellipsoids. The authors found that the theory gave good results even in the dense regime where kinetic theories, which neglect correlated collisions, are not expected to be accurate.

In a gas of inelastic particles, energy is not conserved in particle collisions. It was shown (Kumaran 2004) that it is appropriate to treat energy as a conserved (non-conserved) variable if the length scale of perturbations is smaller (larger) than the 'conduction length', which is obtained as follows. If $e_n$ is the coefficient of restitution, the energy dissipated in a collision between two particles is $O((1-e_n)T)$, where the 'granular temperature' $T$ is the mean square velocity of the particles (the particle mass is assumed to be 1 without loss of generality). It can be inferred, by examining the energy balance equation, that fluctuations in energy are damped over a length scale comparable to $\lambda/(1-e_n)^{1/2}$, where $\lambda$ is the mean free path. The rate of diffusion of energy in the energy balance equation scales as $O(D_T T/L^2)$, where the thermal diffusivity $D_T \sim \lambda T^{1/2}$ in the kinetic theory of gases, while the rate of dissipation of energy is $O((1-e_n)T^{3/2}/\lambda)$, since $(T^{1/2}/\lambda)$ is the frequency of collisions. Equating these two terms, it is clear that the rate of diffusion and rate of dissipation are of equal magnitude when the length scale is comparable to the conduction length defined as $L_c = \lambda/(1-e_n)^{1/2}$. Here, we restrict attention to the 'adiabatic' limit ($L \gg L_c$), where the rate of conduction of energy is small compared to the rates of production and dissipation, and there is a local balance between the rates of production due to shear and dissipation due to inelastic collisions. The conduction of energy is important only in a region of thickness comparable to the conduction length near the walls. It should be noted that the sum of the angular momenta of the particles in a reference frame located at the particle centres is not conserved in a collision, and perturbations to the angular momentum decay over time scales comparable to the inverse of the collision frequency, or over length scales comparable to the mean free path. The constitutive relations in the adiabatic limit for granular flows of smooth inelastic particles were derived in Kumaran (2004). Here, we derive the constitutive relations for rough particles, in order to examine the effect of particle rotation on the constitutive relations.

The constitutive relations, correct to Burnett order, are derived using an expansion in the parameter $\varepsilon$. Though the terms 'Navier–Stokes' and 'Burnett' are used here, it should be noted that the procedure used here is qualitatively different from that used for deriving macroscopic equations in the kinetic theory of gases. In that case, the mean free path $\lambda$ is small compared to the length scale of the flow $L$, and the mean velocity $U$ is small compared to the root mean square velocity of the gas $T^{1/2}$, so that an expansion is used in the gradients of the density, velocity and temperature. The number of spatial derivatives in the Burnett terms in the stress tensor is one higher than that in the Newton's law of viscosity. In the present case, an expansion is carried out in the small parameter $\varepsilon = (1-e_n)^{1/2}$, which represents the departure from elastic (energy conserving) collisions. In this expansion, the leading-order contribution to the stress tensor is the isotropic pressure, the $O(\varepsilon)$ correction provides Newton's law for viscosity, while the $O(\varepsilon^2)$ correction provides the 'Burnett' terms.

Two models for particle interactions are considered here. In the case of rough particles, the relative tangential velocity after collision is $-e_t$ times the relative tangential velocity before collision, and the coefficient of restitution $e_t$ is $(1-O(\varepsilon^2))$. In an $\varepsilon$ expansion, terms proportional to $\varepsilon$ are neglected in the leading approximation,

and the relative tangential velocity at contact is reversed in a collision, leading to energy conservation. A deficiency of the rough particle model is that the relative tangential velocity at contact is reversed even for a grazing collision, for which there is very little collisional impulse along the line joining the centres. A more realistic model, which is the partially rough particle model, is also analysed here. In the partially rough particle model, the collision is considered to be rough if the angle between the line joining the centres and the relative velocity is less than the 'roughness angle', and smooth if the angle between the line joining the centres and the relative velocity is greater than the roughness angle. For simplicity, the roughness angle is considered to be $(\pi/4)$ in the present analysis, though other values of the roughness angle can be analysed using a similar procedure. This model has the advantage that head-on collisions are rough whereas grazing collisions are smooth. Energy is conserved in the leading approximation in this case as well. Another model used previously in literature is the 'frictional particle' model, in which the contact during a collision could be of two types (Herbst, Huthmann & Zippelius 2000; Jenkins & Zhang 2002). The first is the 'sliding contact' in which the tangential impulse between colliding particles is given by the Coulomb friction law if the angle between the relative velocity vector and the line joining the centres is greater than a 'friction angle' $\theta_f$. The second is 'sticking collisions', for which the tangential coefficient of restitution is a constant, when the angle between the relative velocity and the line joining the centres is less than $\theta_f$. As discussed in Herbst *et al.* (2000), for a frictional collision, the energy loss in a collision is small compared to the sum of the energies of the particles only in two limits. The first is the smooth particle limit, where the tangential coefficient of restitution is close to $-1$ and the coefficient of friction is small. In this limit, constitutive relations correct to $O(\varepsilon)$ were derived by Jenkins & Zhang (2002), and it was found that the stress and the translational component of the temperature are identical to those for smooth particles in the Navier–Stokes approximation, though there is an additional contribution to the energy dissipation owing to particle friction. In a similar manner, the results of the present calculation indicate that the Burnett-order terms in the equation for the stress tensor are also identical to those for smooth particles, though there is an additional contribution to the energy dissipation owing to the friction of the particles. Consequently, this limit is not examined in detail in the present analysis. The second limit is for $\theta_f \to (\pi/2)$ and $\mu_f \to \infty$ for sliding collisions and $e_t \to 1$ for sticking collisions. The constitutive relation derived correct to Burnett order for frictional particles, using a procedure similar to that used here, is identical to that for rough particles, though there is an additional contribution to the energy dissipation owing to friction. Consequently, the details of this calculation are not provided.

In the kinetic theory of gases, the Burnett coefficients can be calculated only in the dilute limit, where the assumption of molecular chaos is valid. If the shear stress is expanded as a function of the strain rate $\dot{\gamma}$ for a linear shear flow, the leading (Navier–Stokes) term is proportional to $\dot{\gamma}$, while the next higher 'Burnett' term, is proportional to $\dot{\gamma}^2$. When the number density increases, there is a contribution to the stress owing to correlations in the particle positions prior to collision (Ernst *et al.* 1978) which are incorporated in the 'ring kinetic equation'. The leading correction to the stress due to correlated collisions is proportional to $|\dot{\gamma}|^{3/2}$, which is large compared to the Burnett terms in the limit $\dot{\gamma} \to 0$, so that the Burnett coefficients diverge in this case. For a granular flow, the temperature and the rate of deformation are related, since the rate of deformation is the source of energy which sustains the fluctuating velocity of the particles. An asymptotic analysis in the parameter $\varepsilon = (1 - e_n)^{1/2}$ is

used in the present analysis, and the ratio $(\dot{\gamma}/T^{1/2}) \propto \varepsilon\lambda^{-1}$, where $\lambda$ is the mean free path, so that the non-analytic correction to the Burnett coefficients is significant for $(k\lambda) > \varepsilon^{1/2}$. However, the calculation of the Burnett coefficients is restricted to the low-wavenumber regime $(k\lambda) \ll \varepsilon$, or $(\dot{\gamma}/T^{1/2}) \gg k$ and the regular Burnett expansion is valid in this limit.

The present analysis is more comprehensive than the kinetic theory analysis of Pidduck (1924) because it is not restricted to the low-density regime. In addition, the Burnett coefficients in the equation for the stress tensor are determined here, whereas the earlier studies of Pidduck (1924) and Theodosopolou & Dahler (1974*a*,*b*) for elastic spheres and Lun & Savage (1987) and Lun (1991) for inelastic spheres were restricted to the viscometric coefficients in Newton's law for viscosity. We use a perturbation expansion in the small parameter $\varepsilon = (1 - e_n)^{1/2}$, and formulate balance equations for only the conserved fields, which are the mass and momentum fields. The angular momentum and energy fields, which are not conserved, are determined as a function of the rate of deformation. This is simpler than the analysis of Lun & Savage (1987) and Lun (1991) where fields for the angular momentum and the translational and rotational energies were included in the description, and this simplification enables the calculation of the Burnett coefficients in the expression for the stress tensor. The expression for the shear viscosity calculated here turns out to be slightly different from that of Pidduck (1924), because of a slight difference in the calculation procedure, and this difference is explained in Appendix A.

The constitutive relations are used to examine the variation of volume fraction with the angle of inclination for the steady 'bulk' flow of granular material down an inclined plane. Pouliquen (1999) experimentally studied the chute flow of a granular material down a rough inclined plane. This study indicated that there is inception of flow only when the angle of inclination of the base with respect to the horizontal exceeds a minimum angle, and there is steady fully developed flow only when the angle of inclination is between a minimum and a maximum value. The mean velocity was found to increase as $h^{3/2}$, where $h$ is the layer height; this scaling is expected if the stress is due to instantaneous collisions and the Bagnold law is used for the stress as a function of strain rate (Silbert *et al.* 2001), though earlier studies have reported an increase proportional to $h^{1/2}$ when the stress is the sum of a kinetic part due to instantaneous collisions and a frictional part due to enduring contacts (Louge & Keast 2001). The other significant result was the correlation between the average velocity during flow, and the height of the layer after cessation of flow $h_{stop}$. Though $h_{stop}$ was typically much smaller than the height of the material during flow, the correlation between these indicates that the same microscopic properties are responsible both for the average velocity during flow and for determining the minimum height at which flow stops.

Silbert *et al.* (2001) carried out large-scale simulations of the flow of granular material down an inclined plane. Detailed profiles were obtained for the velocity and the fluctuating energy. The broad features of the flow were similar to those in the experiments of Pouliquen (1999), and it was observed that the flow inception occurs at a minimum angle of inclination and that the flow becomes unstable and continually accelerates beyond a maximum angle of inclination. One of the significant observations of the study was that the constitutive relation for the stress is given by the Bagnold law, which states that the stress is proportional to the square of the strain rate. Pouliquen & Chevoir (2002) compared the ratio of the stress and strain rate, as well as the shear and normal stresses, for two different configurations, the flow down an inclined plane and the shear flow between two parallel plates. They observed that

the ratio of the shear and normal stresses, as well as the dependence of the stresses on the strain rate, were identical in both cases, indicating that the constitutive relation at the microscopic scale is identical in both cases.

A model for the granular flow down a plane, based on kinetic theory, was formulated by Louge (2003). The flow was divided into a 'core region' away from the bottom boundary where the density is nearly a constant, a 'basal layer' near the bottom surface and a 'surface layer' near the top surface. The density is nearly a constant in the 'core region', while it increases slightly near the bottom and decreases to zero in the surface layer. The stress was separated into a kinetic part due to instantaneous collisions, and a frictional part due to enduring contacts. The frictional part was assumed to satisfy the Coulomb law of friction, while the kinetic part was modelled using kinetic theory. The ratio of the kinetic and frictional part of the stress tensor, when inserted into the energy balance equation, resulted in a minimum angle required for the inception of flow. One drawback of this model is that the density in the core region cannot be explicitly determined, and a model based on the simulations of Silbert *et al.* (2001) was used. The model of Bocquet, Errami & Lubensky (2002) was based on the momentum equation which relates the pressure gradient to the weight, and the heat conduction equation for the fluctuating energy of the particles. Numerical solutions of the model equations showed many of the features observed in the simulations.

The simulations of Silbert *et al.* (2001) have provided a large amount of detail about the configuration, velocity and stress profiles for the flow down an inclined plane. One of the striking features is the remarkable constancy of the volume fraction in the bulk of the flow. In addition, the fact that the stress and velocity profiles obey Bagnold scaling suggests that a kinetic theory approach may work for this case. The Bagnold law for the stress is a dimensional necessity if the only time scale in the problem is the inverse of the strain rate, and there are no material time scales. The validity of Bagnold law suggests that there are no time scales in the problem relating to the particle interactions, and that particle interactions can be modelled using dimensionless parameters. There are two types of model where particle interactions can be modelled by dimensionless parameters: the 'quasi-static' model which provides a relation between the normal and tangential forces at contact; and the kinetic model which assumes that the interaction between particles is due to instantaneous collisions. Clearly, the quasi-static model is not applicable to the simulations of Silbert *et al.* (2001), since the particles do not remain in extended contact, and the instantaneous coordination number varies between 1 and 2 in most cases. This suggests that the flow can be successfully modelled using a kinetic approach. The analysis in § 3 suggests that this is indeed the case.

The viscometric coefficients in the Burnett approximation for rough and partially rough particles are evaluated in the next section. These are then used to determine the density as a function of the angle of inclination in § 3 for the flow down an inclined plane. The important conclusions of the analysis are summarized in § 4.

## 2. Constitutive relations

The system consists of rough inelastic spheres of diameter $d$ subjected to a two-dimensional deformation field $G_{ij} = (\partial U_i/\partial x_j)$, where $U_i$ is the mean velocity, and indicial notation is used to represent vectors and tensors. The particle mass $m$ and diameter $d$ are set equal to 1 without loss of generality, so that all mass and length dimensions are non-dimensionalized by the particle mass and diameter, respectively.

The motion of the particles is described by their velocity $u_i$ and the angular velocity $\omega_i$. The fluctuating velocity of the particles is defined as $\boldsymbol{c} = \boldsymbol{u} - \boldsymbol{U}$, while the fluctuating angular velocity is defined as $\varpi = \omega - \boldsymbol{\Omega}$, where $\boldsymbol{\Omega}$ is the mean angular velocity. Note that $\boldsymbol{U}$ is a linear function of depth, since the strain rate is assumed to be a constant over distances comparable to the mean free path, while $\boldsymbol{\Omega}$ is independent of position for a homogeneous shear flow. The distribution function $f(\boldsymbol{x}, \boldsymbol{c}, \varpi, t)$ is defined such that $f(\boldsymbol{x}, \boldsymbol{c}, \varpi, t)\,\mathrm{d}\boldsymbol{c}\,\mathrm{d}\varpi$ is the probability of finding a particle at location $\boldsymbol{x}$ and time $t$ in the differential volume $\mathrm{d}\boldsymbol{c}$ about $\boldsymbol{c}$ in velocity space having angular velocity in the interval $\mathrm{d}\varpi$ about $\varpi$. The Boltzmann equation for the distribution function is given by

$$\frac{\mathrm{D}(\rho f)}{\mathrm{D}t} + \frac{\partial(\rho c_i f)}{\partial x_i} + \left(a_i - \frac{\mathrm{D}U_i}{\mathrm{D}t}\right)\frac{\partial(\rho f)}{\partial c_i} - G_{ij}c_j\frac{\partial(\rho f)}{\partial c_i} = \frac{\partial_c(\rho f)}{\partial t}, \tag{2.1}$$

where indicial notation is used to represent vectors and a repeated index implies a dot product. In equation (2.1), $\rho$ is the number density of the particles, $\boldsymbol{a}$ is the particle acceleration due to body forces, and $(\mathrm{D}/\mathrm{D}t) \equiv (\partial/\partial t) + U_i(\partial/\partial x_i)$ is the substantial derivative. The second and third terms on the left-hand side of (2.1) are the rates of change of the distribution function due to the motion of the particles in real space and the motion in velocity space due to the acceleration of the particles. The fourth term on the left-hand side is the rate of change of the distribution function due to the change in the mean velocity with spatial position. The term on the right-hand side is the rate of change of the distribution function due to particle collisions. Though equation (2.1) appears to differ from the standard form used in the literature, it is easily obtained when the particle velocity is expressed as the sum of the mean and fluctuating velocity, as shown in Chapman & Cowling (1970).

The linear and angular velocity distributions in a homogeneous flow at steady state are assumed to be of the form $f(\boldsymbol{x}, \boldsymbol{c}, \varpi, t) = f_c(\boldsymbol{c})f_\omega(\varpi)$, where

$$f_c(\boldsymbol{c}) = \frac{1}{(2\pi)^{3/2}\sqrt{\mathrm{Det}(\boldsymbol{T})}}\exp\left(-\frac{c_i T_{ij}^{-1} c_j}{2}\right), \tag{2.2}$$

$$f_\omega(\varpi) = \frac{1}{(2\pi)^{3/2}\sqrt{\mathrm{Det}(\boldsymbol{\Upsilon})}}\exp\left(-\frac{\varpi_i \Upsilon_{ij}^{-1} \varpi_j}{2}\right), \tag{2.3}$$

where $T_{ij} = \langle c_i c_j \rangle$ is the second-order tensor of second moments of the velocity distribution function, and $\Upsilon_{ij} = \langle \varpi_i \varpi_j \rangle$ is the second-order tensor of the second moments of the angular velocity fluctuations, where the average $\langle \star \rangle$ of a moment $\star$ is defined as

$$\langle \star \rangle = \int \mathrm{d}\boldsymbol{c} \int \mathrm{d}\varpi f(\boldsymbol{x}, \boldsymbol{c}, \varpi, t)\,\star. \tag{2.4}$$

The second moments $T_{ij}$ and $\Upsilon_{ij}$ are determined from conservation equations for the second moments of the velocity distribution, $\langle c_i c_j \rangle$, and the first and second moments of the angular velocity distribution, $\langle \omega_i \rangle$ and $\langle \varpi_i \varpi_j \rangle$,

$$\rho\frac{\mathrm{D}T_{ij}}{\mathrm{D}t} + \rho(G_{ik}T_{kj} + G_{jk}T_{ki}) = \frac{\partial_c \rho \langle c_i c_j \rangle}{\partial t}, \tag{2.5}$$

$$\rho\frac{\mathrm{D}\Omega_i}{\mathrm{D}t} = \frac{\partial_c(\rho\omega_i)}{\partial t}, \tag{2.6}$$

$$\rho\frac{\mathrm{D}(\Upsilon_{ij} + \Omega_i\Omega_j)}{\mathrm{D}t} = \frac{\partial_c(\rho\omega_i\omega_j)}{\partial t}. \tag{2.7}$$

In equations (2.5), (2.6) and (2.7), the mass conservation condition $(\mathrm{D}\rho/\mathrm{D}t)+\rho G_{ii}=0$ has been used to simplify the expressions on the left-hand side. It should be noted that $T_{ij}$ and $\Upsilon_{ij}$ are functions of $\varepsilon$, and these are determined using an expansion in $\varepsilon$ in equation (2.14). This form of the distribution function was used to obtain constitutive relations for smooth inelastic particles by Kumaran (2004), and it was found that the results are identical to those of the Chapman–Enskog procedure (Chapman & Cowling 1970) if only the first term in the Sonine-polynomial expansion for the distribution function is retained. In addition, it was found that the errors are numerically small even when the higher-order terms in the expansion are included. In the present analysis, we verify that the results for the pressure and viscosity are identical to those obtained by the Chapman–Enskog procedure for rough particles when the leading term in the Sonine-polynomial expansion is retained.

The collision rules used for calculating the collision integral are as follows. Consider a collision between two particles having velocities $u_i$ and $u_i^*$, and angular velocities $\omega_i$ and $\omega_i^*$, in which the unit vector in the direction of the line joining the centres of the particles from the particle at $\boldsymbol{x}$ to the particle at $\boldsymbol{x}^*$ is $\boldsymbol{k}$. In a collision that conserves linear and angular momenta, the sum of the velocities $(u_i+u_i^*)$ and the difference in the angular velocities $(\omega_i-\omega_i^*)$ are conserved in the collision. The velocity difference between the two particles at the point of contact is $g_i=(u_i-u_i^*)-(\epsilon_{ijl}/2)k_j(\omega_l+\omega_l^*)$. The components of the relative velocity parallel and perpendicular to the line joining the centres of the particles are,

$$\begin{aligned} g_ik_i &= (u_i-u_i^*)k_i \\ &= c_i^{(-)}k_i - k_iG_{ij}k_j, \end{aligned} \tag{2.8}$$

$$\begin{aligned} (\delta_{ij}-k_ik_j)g_j &= (\delta_{ij}-k_ik_j)(u_j-u_j^*)+(\epsilon_{ijl}/2)k_j(\omega_l+\omega_l^*) \\ &= (\delta_{ij}-k_ik_j)\left(c_j^{(-)}-G_{jk}k_k\right)+(\epsilon_{ijl}/2)k_j\omega_l^{(+)}, \end{aligned} \tag{2.9}$$

where $c_i^{(-)}=c_i-c_i^*$ is the difference in the fluctuating velocities of the particles, $\omega_i^{(+)}=\omega_i+\omega_i^*$ is the sum of the angular velocities, $k_i$ is the unit vector in the direction of the line joining the centres of the particles, and $\epsilon_{ijl}$ is the invariant antisymmetric tensor. In the collisional model used here, the post-collisional tangential and normal velocities are related to their pre-collisional values by

$$g_i'k_i = -e_ng_ik_i, \tag{2.10}$$

$$(\delta_{ij}-k_ik_j)g_j' = -e_t(\delta_{ij}-k_ik_j)g_j, \tag{2.11}$$

where $0\leqslant e_n\leqslant 1$ and $-1\leqslant e_t\leqslant 1$ are the normal and tangential coefficients of restitution. In the direction along the line joining centres, $e_n=1$ corresponds to elastic collisions and $e_n=0$ corresponds to perfectly inelastic collisions, while in the direction normal to the line joining the centres, $e_t=-1$ corresponds to smooth spheres and $e_t=1$ corresponds to rough spheres for which the relative tangential velocity vector changes sign upon collision. Using these collision laws, it is shown in Appendix B that the post-collisional linear and angular velocities are related to their pre-collisional values by

$$\begin{aligned} u_i'-u_i = &-((1+e_n)/2)(u_j-u_j^*)k_jk_i-((1+e_t)/2)(4\mathscr{I}/(1+4\mathscr{I}))((\delta_{ij}-k_ik_j)(u_j-u_j^*), \\ &-(\epsilon_{ijl}/2)k_j(\omega_l+\omega_l^*)) \end{aligned} \tag{2.12}$$

$$\omega_i'-\omega_i = -((1+e_t)/2)(4\mathscr{I}/(1+4\mathscr{I}))(1/2\mathscr{I})(\epsilon_{ijl}k_j(u_l-u_l^*)+(1/2)(\delta_{ij}-k_ik_j)(\omega_j+\omega_j^*)), \tag{2.13}$$

where $\mathscr{I}$ is the moment of inertia scaled by the product of the mass and the square of the diameter of the particle. It is natural to use an expansion in the small parameter $e_n = (1 - \varepsilon^2)$ (Kumaran 2004), so that the rate of dissipation of energy is given, correct to leading order in small $\varepsilon$, by $4\sqrt{\pi}\rho^2\chi T^{3/2}\varepsilon^2$ for smooth spheres. The collision integrals can be evaluated using an expansion in the parameter $\varepsilon$. The resulting expressions, which are explicitly functions of the parameters $\mathscr{I}$, are algebraically complicated, and so these are not provided in detail. In the present study, three different models for particle collisions are considered,

(i) Smooth inelastic particles for which $(1-e_n) = \varepsilon^2 \ll 1$ and $e_t = -1$, so that there is no change in the angular velocities in a collision. These have already been analysed (Kumaran 2004), and so are not analysed in detail here. In this case, the rate of dissipation of energy, correct to leading order in $\varepsilon$, is given by $4\sqrt{\pi}\rho^2\chi T^{3/2}\varepsilon^2$.

(ii) Rough inelastic particles are those with $e_n \to 1$ and $e_t \to 1$, so that $(1 - e_n) = \varepsilon^2 \ll 1$. The rate of dissipation of energy is given by $2\sqrt{\pi}\rho^2\chi T^{3/2}((1-e_n^2)+(1-e_t^2))$. In this case, the dissipation due to the translational and rotational modes are comparable only when $(1 - e_t) \sim \varepsilon^2$. The substitution $(1 - e_t^2) = 2a_t\varepsilon^2$, is used where $a_t = (1 - e_t^2)/(1 - e_n^2)$ is a numerical $O(1)$ factor. The rate of dissipation of energy is then given by $4\sqrt{\pi}\varepsilon^2\rho^2\chi T^{3/2}(1 + a_t)$.

(iii) Partially rough particles are those with $(1 - e_n) = \varepsilon^2 \ll 1$, and $e_t = -1$ if the angle between the relative velocity and the line joining the centres of the particles is greater than the 'roughness angle' (grazing collisions), and $e_t \to 1$ if the angle between the relative velocity and the line joining the centres is less than the 'roughness angle' (head-on collisions). The roughness angle is chosen to be equal to $(\pi/4)$ in the present analysis, though the same procedure can be used for other roughness angles as well. The rate of dissipation of energy is given by $2\sqrt{\pi}\rho^2\chi T^{3/2}((1-e_n^2)+(1-e_t^2)/4)$, which is equivalent to $4\sqrt{\pi}\rho^2\chi T^{3/2}\varepsilon^2(1 + a_t/4)$, where $a_t$ is defined above.

As explained in § 1, the $O(\varepsilon)$ correction to the distribution function is used to obtain the Navier–Stokes terms in the stress tensor which are linear functions of the strain rate, while the $O(\varepsilon^2)$ correction is used to obtain the Burnett coefficients which are quadratic functions of the strain rates. The next higher correction to the stress, due to the $O(\varepsilon^3)$ contribution to the stress tensor, results in corrections to the shear and bulk viscosity coefficients. Here, the expansion is truncated at $O(\varepsilon^2)$, and since there are no corrections to the Navier–Stokes terms due to the $O(\varepsilon^2)$ correction to the distribution function, it is permissible to set $\varepsilon = 0$ while calculating the Navier–Stokes and Burnett contributions to the stress tensor.

The mean square velocities and the mean angular velocity are evaluated using an expansion in the parameter $\varepsilon$,

$$\left.\begin{aligned} T_{ij} &= T_{ij}^{(0)} + \varepsilon T_{ij}^{(1)} + \varepsilon^2 T_{ij}^{(2)}, \\ \Omega_i &= \Omega_i^{(0)} + \varepsilon \Omega_i^{(1)} + \varepsilon^2 \Omega_i^{(2)}, \\ \Upsilon_{ij} &= \Upsilon_{ij}^{(0)} + \varepsilon \Upsilon_{ij}^{(1)} + \varepsilon^2 \Upsilon_{ij}^{(2)}. \end{aligned}\right\} \tag{2.14}$$

In the leading approximation, the source and dissipation of energy are neglected, and the system reduces to a gas of particles at equilibrium in the absence of deformation. For rough particles, there is an equipartition of energy between the translational and rotational degrees of freedom, and the leading-order mean square velocity and angular velocity are given by

$$\left.\begin{aligned} T_{ij}^{(0)} &= T\delta_{ij}, \\ \Upsilon_{ij}^{(0)} &= \Upsilon\delta_{ij}, \end{aligned}\right\} \tag{2.15}$$

where $\Upsilon = (T/\mathscr{I})$. The value of $T$ is determined from a balance between the rates of production and dissipation of energy. A simple energy balance argument (Kumaran 2004) can be used to show that $G_{ij} \sim \varepsilon T^{1/2}$, so that all terms containing the mean strain rate can also be expanded in a series in $\varepsilon$.

The collisional rates of change of the second moments of the linear and angular velocities are calculated as follows. Consider a collision between two particles with fluctuating linear velocities $\boldsymbol{c}$ and $\boldsymbol{c}^*$, and angular velocities $\omega$ and $\omega^*$, such that the velocity of one of the particles transforms from $\boldsymbol{c} \to \boldsymbol{c}'$ and $\omega \to \omega'$. The rate of change of a velocity dependent dynamical variable $\star$ due to collisions is given by

$$\frac{\partial_c \langle \star \rangle}{\partial t} = \rho(\boldsymbol{x}^*)\chi(\phi) \int_{\boldsymbol{c},\boldsymbol{c}^*} \int_{\boldsymbol{\omega},\boldsymbol{\omega}^*} \int_{\boldsymbol{k}} f_c(c_i) f_c(c_i^*) f_\omega(\omega_i) f_\omega(\omega_i^*)(\star' - \star)(u_i - u_i^*)k_i, \qquad (2.16)$$

where $\chi$ is the pair distribution function,

$$\int_{\boldsymbol{c},\boldsymbol{c}^*} \equiv \int \mathrm{d}\boldsymbol{c} \int \mathrm{d}\boldsymbol{c}^*, \quad \int_{\boldsymbol{\omega},\boldsymbol{\omega}^*} \equiv \int \mathrm{d}\boldsymbol{\omega} \int \mathrm{d}\boldsymbol{\omega}^*, \quad \int_{\boldsymbol{k}} \equiv \int \mathrm{d}\boldsymbol{k},$$

$\boldsymbol{k}$ is the unit vector along the line joining the centres of the particles, $(u_i - u_i^*) = c_i - c_i^* - G_{ij}k_j$ is the difference in the total velocity of the two particles (the difference in mean velocities is $-G_{ij}k_j$ where $G_{ij}$ is the mean strain rate), and the $\boldsymbol{k}$ integral is carried out for $\boldsymbol{k}\cdot(\boldsymbol{u} - \boldsymbol{u}^*) > 0$, so that the particles approach prior to collision. In order to evaluate the collision integral, the distribution functions are first expressed in a series in the parameter $\varepsilon$ using the expansions (2.14) for $T_{ij}$ and $\Upsilon_{ij}$,

$$f_c(\boldsymbol{c}) = F_c(\boldsymbol{c})\big(1 + \varepsilon\Phi_c^{(1)}(\boldsymbol{c}) + \varepsilon^2\Phi_c^{(2)}(\boldsymbol{c})\big), \qquad (2.17)$$

$$f_\omega(\boldsymbol{\omega}) = F_\omega(\boldsymbol{\omega})\big(1 + \varepsilon\Phi_\omega^{(1)}(\boldsymbol{\omega}) + \varepsilon^2\Phi_\omega^{(2)}(\boldsymbol{\omega})\big), \qquad (2.18)$$

where

$$F_c(\boldsymbol{c}) = \left(\frac{1}{2\pi T}\right)^{3/2} \exp\left(-\frac{c_i^2}{2T}\right), \qquad (2.19)$$

$$F_\omega(\boldsymbol{\omega}) = \left(\frac{1}{2\pi \Upsilon}\right)^{3/2} \exp\left(-\frac{\varpi_i^2}{2\Upsilon}\right), \qquad (2.20)$$

$\Phi_c^{(1)}$ and $\Phi_\omega^{(1)}$ are functions of $T_{ij}^{(1)}$ and $\Upsilon_{ij}^{(1)}$, respectively, and $\Phi_c^{(2)}$ and $\Phi_\omega^{(2)}$ are functions of $(T_{ij}^{(1)}, T_{ij}^{(2)})$ and $(\Upsilon_{ij}^{(1)}, \Upsilon_{ij}^{(2)})$, respectively.

The products of the velocity distribution functions in the integral (2.16) are simplified as follows. The particle velocities are expressed in terms of the sum of the velocities $\boldsymbol{c}^{(+)} = \boldsymbol{c} + \boldsymbol{c}^*$, and the velocity difference $\boldsymbol{c}^{(-)} = \boldsymbol{c} - \boldsymbol{c}^*$,

$$F_c(\boldsymbol{c})F_c(\boldsymbol{c}^*) = F_{c^{(+)}}\big(\boldsymbol{c}^{(+)}\big)F_{c^{(-)}}\big(\boldsymbol{c}^{(-)}\big), \qquad (2.21)$$

where

$$F_{c^\pm}(\boldsymbol{c}^\pm) = \left(\frac{1}{4\pi T}\right)^{3/2} \exp\left(-\frac{c_i^{\pm 2}}{4T}\right). \qquad (2.22)$$

Similarly, the functions $\Phi_c^{(1)}$ and $\Phi_c^{(2)}$ are also expressed in terms of $\boldsymbol{c}^{(+)}$ and $\boldsymbol{c}^{(-)}$. In a similar fashion, the product of the distribution function for the angular velocities,

$$F_\omega(\omega)F_\omega(\omega^*) = F_{\omega^{(+)}}\big(\boldsymbol{\omega}^{(+)}\big)F_{\omega^{(-)}}\big(\boldsymbol{\omega}^{(-)}\big), \qquad (2.23)$$

where $\omega^{(+)} = \omega + \omega^*$ and $\omega^{(-)} = \omega - \omega^*$, and

$$F_{\omega^{\pm}}(\omega^{\pm}) = \left(\frac{1}{4\pi T}\right)^{3/2} \exp\left(-\frac{\omega_i^{\pm 2}}{4T}\right). \tag{2.24}$$

Since the sum of the linear velocities, $\boldsymbol{c}^{(+)}$, remains unchanged in a collision, the integral over $\boldsymbol{c}^{(+)}$ is carried out explicitly. A similar simplification cannot be carried out for $\boldsymbol{c}^{(-)}$ owing to the restriction $(u_i - u_i^*)k_i > 0$ for the particles to approach before a collision.

The distribution function $F_{c^{(-)}}$ is expressed in terms of the total velocity difference before collision, $(\boldsymbol{u} - \boldsymbol{u}^*) = \boldsymbol{c}^{(-)} - \boldsymbol{G}\cdot k$, where $-\boldsymbol{G}\cdot k$ is the difference in the mean velocities of the two particles.

$$F_{c^{(-)}}(\boldsymbol{c}^{(-)}) = \left(\frac{1}{4\pi T}\right)^{3/2} \exp\left(-\frac{(u_i - u_i^* - G_{ij}k_j)^2}{4T}\right). \tag{2.25}$$

In the above equation $(\boldsymbol{u} - \boldsymbol{u}^*)$ is $O(T^{1/2})$, while a simple energy balance can be used to show that $\boldsymbol{G} \sim \varepsilon T^{1/2}$. Therefore, the distribution function $F_{c^{(-)}}$ can be expressed in a series in $\varepsilon$, and the integral over the total velocity difference $(\boldsymbol{u} - \boldsymbol{u}^*)$ and the direction of the line joining the centres of the particles $k_i$ can be evaluated.

### 2.1. *Rough particles*

The calculation of the mean angular velocity is carried out in detail, in order to illustrate the procedure used for the calculations, but the details of the calculations for pressure, viscosity and the Burnett coefficients are not explained, and only the final results are provided. For the purpose of calculation, the rate of deformation tensor is expressed as

$$G_{ij} = S_{ij} + A_{ij} + (\delta_{ij}/3)G_{kk}, \tag{2.26}$$

where $S_{ij} = (1/2)(G_{ij} + G_{ji} - (2\delta_{ij}/3)G_{kk})$ is the symmetric traceless part of the rate of deformation tension, $A_{ij} = (1/2)(G_{ij} - G_{ji})$ is the antisymmetric part of the rate of deformation tensor, and the identity tensor $\delta_{ij}$ is defined such that $\delta_{ij} = 1$ for $i = j$, and $\delta_{ij} = 0$ for $i \neq j$. The rate of change of the mean angular momentum due to inter-particle collisions, including terms that are quadratic in the rate of deformation tensor, is

$$\begin{aligned}\frac{\partial_c \rho \langle \omega_i \rangle}{\partial t} = \rho^2 \chi(\phi) \mathscr{J}\mathscr{K} \Bigg[ & -\frac{2\sqrt{\pi}(2\Omega_i + \epsilon_{ijk}A_{jk})}{3} + \frac{2\pi\Omega_i G_{jj}}{9T^{1/2}} - \frac{2\pi S_{ij}\Omega_j}{15T^{1/2}} + \frac{2\varepsilon\sqrt{\pi}T_{ij}^{(1)}\Omega_j}{15T^{1/2}} \\ & + \frac{2\pi\epsilon_{ijk}A_{jk}G_{ll}}{15} - \frac{\pi S_{ij}\epsilon_{jkl}A_{kl}}{15} - \frac{2\sqrt{\pi}\varepsilon\epsilon_{ijk}T_{jl}^{(1)}G_{lk}}{15} \\ & - \frac{8\sqrt{\pi}\varepsilon\Omega_i T_{jj}^{(1)}}{5} - \frac{11\sqrt{\pi}\varepsilon\epsilon_{ijk}A_{jk}T_{ll}^{(1)}}{15} \Bigg],\end{aligned} \tag{2.27}$$

where $\mathscr{K} = (1/2\mathscr{I})$, $\mathscr{J} = (4\mathscr{I}(1 + e_t)/(1 + 4\mathscr{I}))$. This is inserted into equation (2.6) and solved to obtain the mean angular velocity as a function of the local rate of deformation. The mean angular velocity is expanded in a series in the parameter $\varepsilon$, $\Omega_i = \Omega_i^{(0)} + \varepsilon\Omega_i^{(1)}$, and inserted into equation (2.6). The leading-order solution for the angular velocity, which is a linear function of the rate of deformation, is half the local vorticity,

$$\Omega_i^{(0)} = -\frac{\epsilon_{ijk}A_{jk}}{2}. \tag{2.28}$$

This is inserted into equations (2.6) and (2.27) to obtain the first correction to the angular velocity,

$$\varepsilon\Omega_i^{(1)} = \frac{-3}{4\sqrt{\pi}\mathscr{J}\mathscr{K}\rho^2\chi(\phi)}\frac{\mathrm{D}\Omega_i^{(0)}}{\mathrm{D}t}, \tag{2.29}$$

where $\mathscr{K} = (1/2\mathscr{I})$, $\mathscr{J} = (4\mathscr{I}(1+e_t)/(1+4\mathscr{I}))$. The result $T_{ij}^{(1)} = -Q_T T^{1/2} S_{ij} - Q_{TI} T^{1/2}\delta_{ij} G_{kk}$, obtained later in equations (2.36) and (2.45), has been used in deriving equation (2.29). The substantial derivative of the leading contribution to the mean angular velocity on the right-hand side of equation (2.29) is simplified as indicated in Appendix C,

$$\frac{\mathrm{D}\Omega_i^{(0)}}{\mathrm{D}t} = +\frac{\epsilon_{ijk}}{2}\left(\partial_k\left(\frac{\partial_j p}{\rho}\right) - \partial_j\left(\frac{\partial_k p}{\rho}\right)\right) + \epsilon_{ijk}(A_{jl}S_{lk} + S_{jl}A_{lk}), \tag{2.30}$$

where the pressure $p$ is defined in equation (2.56) below. This is used to obtain the angular velocity, correct to second order in the rate of deformation tensor,

$$\Omega_i = -\frac{\epsilon_{ijk}A_{jk}}{2} - \frac{3}{4\sqrt{\pi}\mathscr{J}\mathscr{K}\rho^2\chi}\left(\epsilon_{ijk}(A_{jl}S_{lk} + S_{jl}A_{lk}) + \frac{\epsilon_{ijk}}{2}\left(\partial_k\left(\frac{\partial_j p}{\rho}\right) - \partial_j\left(\frac{\partial_k p}{\rho}\right)\right)\right), \tag{2.31}$$

where $\mathscr{K} = (1/2\mathscr{I})$, $\mathscr{J} = (4\mathscr{I}(1+e_t)/(1+4\mathscr{I}))$.

The collision integrals for the second moments of the velocity distribution are inserted into the conservation equations to obtain the first corrections $T_{ij}^{(1)}$ and $\Upsilon_{ij}^{(1)}$. The equation for the deviatoric part of the second moment for the velocity field is

$$\rho T(G_{ij} + G_{ji} - (2/3)\delta_{ij}G_{kk}) = \left.\frac{\partial_c \rho\langle c_i c_j - \delta_{ij}c_k^2/3\rangle}{\partial t}\right|_1, \tag{2.32}$$

where the first correction to the collision integral for the deviatoric part of the second moment of the velocity distribution is

$$\begin{aligned}\left.\frac{\partial_c \rho\langle c_i c_j - \delta_{ij}c_k^2/3\rangle}{\partial t}\right|_1 &= \rho^2\chi\left[T^{1/2}S_{ij}\pi\left[-\frac{8}{15} - \frac{2\mathscr{J}}{3} + \frac{2\mathscr{J}^2}{15} + \frac{\mathscr{J}^2\Upsilon}{30}\right]\right.\\ &\quad + \varepsilon\left(T_{ij}^{(1)} - (\delta_{ij}/3)T_{kk}^{(1)}\right)\sqrt{\pi}\left[-\frac{16}{5} + \frac{4\mathscr{J}^2}{5} - \frac{\mathscr{J}^2\Upsilon}{30T}\right]\\ &\quad \left. - \frac{\varepsilon\sqrt{\pi}\mathscr{J}^2\left(\Upsilon_{ij}^{(1)} - (\delta_{ij}/3)\Upsilon_{kk}^{(1)}\right)}{6}\right].\end{aligned} \tag{2.33}$$

The equation for the deviatoric part of the second moment for the angular velocity field is

$$0 = \left.\frac{\partial_c \rho\langle \omega_i\omega_j - \omega_k^2\delta_{ij}/3\rangle}{\partial t}\right|_1, \tag{2.34}$$

where the first correction to the collision integral for the second moment of the angular velocity distribution is

$$\begin{aligned}\left.\frac{\partial_c\langle \omega_i\omega_j - \omega_k^2\delta_{ij}/3\rangle}{\partial t}\right|_1 &= \rho^2\chi\left[S_{ij}\pi\left[\frac{\mathscr{K}\mathscr{J}(4\mathscr{K}\mathscr{J} + (\mathscr{K}\mathscr{J} - 4)\Upsilon)}{30}\right]\right.\\ &\quad + \varepsilon\left(T_{ij}^{(1)} - (\delta_{ij}/3)T_{kk}^{(1)}\right)\sqrt{\pi}\mathscr{J}\mathscr{K}\left[-\frac{4\mathscr{K}\mathscr{J}}{5} + \frac{2\Upsilon}{15} - \frac{\mathscr{K}\mathscr{J}\Upsilon}{30}\right]\\ &\quad \left. + \frac{\sqrt{\pi}\varepsilon\mathscr{J}\mathscr{K}\left(\Upsilon_{ij}^{(1)} - (\delta_{ij}/3)\Upsilon_{kk}^{(1)}\right)(7\mathscr{J}\mathscr{K} - 40)}{30}\right],\end{aligned} \tag{2.35}$$

where $\mathscr{K} = (1/2\mathscr{I})$, $\mathscr{J} = (4\mathscr{I}(1+e_t)/(1+4\mathscr{I}))$. Equations (2.32) and (2.34) (in which the right-hand sides are given by (2.33) and (2.35), respectively) are simultaneous tensor equations for $T_{ij}^{(1)}$ and $\Upsilon_{ij}^{(1)}$, and the inhomogeneous terms in these equations are both proportional to the tensor $S_{ij}$. Therefore, these can be solved simultaneously to obtain the symmetric traceless parts of $T_{ij}^{(1)}$ and $\Upsilon_{ij}^{(1)}$, both of which are proportional to $S_{ij}$,

$$\left.\begin{aligned}\left(T_{ij}^{(1)} - (\delta_{ij}/3)T_{kk}^{(1)}\right) &= -Q_T S_{ij} T^{1/2},\\ \left(\Upsilon_{ij}^{(1)} - (\delta_{ij}/3)\Upsilon_{kk}^{(1)}\right) &= -Q_\Upsilon S_{ij} T^{1/2},\end{aligned}\right\} \tag{2.36}$$

where the coefficients $Q_T$ and $Q_\Upsilon$, obtained by solving the simultaneous equations (2.32) and (2.34), are

$$\begin{aligned} &Q_T(\mathscr{J}^3\mathscr{K}\Upsilon - 5\mathscr{J}^2\Upsilon - 4\mathscr{J}^3\mathscr{K} + 80\mathscr{J}^2 + 56\mathscr{J}\mathscr{K} - 320)\\ &\quad = (\sqrt{\pi}/3)(160 + 200\mathscr{J} - 28\mathscr{J}\mathscr{K} - 40\mathscr{J}^2 - 35\mathscr{J}^2\mathscr{K} + 12\mathscr{J}^3\mathscr{K} - 15\Upsilon\mathscr{J}^2 + 3\mathscr{J}^3\mathscr{K}\Upsilon)\\ &\qquad + \frac{5\sqrt{\pi}(40 - 7\mathscr{J}\mathscr{K})}{6\phi\chi}, \end{aligned} \tag{2.37}$$

$$\begin{aligned} &Q_\Upsilon(\mathscr{J}^3\mathscr{K}\Upsilon - 5\mathscr{J}^2\Upsilon - 4\mathscr{J}^3\mathscr{K} + 80\mathscr{J}^2 + 56\mathscr{J}\mathscr{K} - 320)\\ &\quad = (\sqrt{\pi}/3)(-192\mathscr{J}\mathscr{K} - 120\mathscr{J}^2\mathscr{K} + 48\mathscr{J}^3\mathscr{K} + 112\Upsilon + 20\mathscr{J}\Upsilon - 28\mathscr{J}\mathscr{K}\Upsilon\\ &\qquad - 28\mathscr{J}^2\Upsilon - 5\mathscr{J}^2\mathscr{K}\Upsilon + 12\mathscr{J}^3\mathscr{K}\Upsilon) + \frac{5\sqrt{\pi}(24\mathscr{J}\mathscr{K} - 4\Upsilon + \mathscr{J}\mathscr{K}\Upsilon)}{6\phi\chi}. \end{aligned} \tag{2.38}$$

For smooth particles in the limit $\mathscr{J} = 0$, $Q_T$ and $Q_\Upsilon$ are

$$Q_T = \left(\frac{\sqrt{\pi}}{6} + \frac{5\sqrt{\pi}}{48\phi\chi}\right), \tag{2.39}$$

$$Q_\Upsilon = \sqrt{\pi}\Upsilon\left(\frac{7}{60} + \frac{1}{96\phi\chi}\right). \tag{2.40}$$

Equation (2.39) is identical to the result derived in for the flow of smooth nearly elastic spheres in Kumaran (2004). In the opposite limit of rough spheres, where $\mathscr{J} = (8\mathscr{I}/(1+4\mathscr{I}))$, $Q_T$ and $Q_\Upsilon$ are

$$Q_T = \frac{\sqrt{\pi}(1+4\mathscr{I})(3+40\mathscr{I})(5+20\mathscr{I}+8\phi\chi+80\mathscr{I}\phi\chi)}{48(3+66\mathscr{I}+280\mathscr{I}^2)\phi\chi}, \tag{2.41}$$

$$Q_\Upsilon = -\frac{5\sqrt{\pi}(1+4\mathscr{I})(5+20\mathscr{I}+8\phi\chi+80\mathscr{I}\phi\chi)}{12(3+66\mathscr{I}+280\mathscr{I}^2)\phi\chi}. \tag{2.42}$$

For a uniform sphere, $\mathscr{I} = 1/10$, and $Q_T$ and $Q_\Upsilon$ are

$$Q_T = \frac{49\sqrt{\pi}(7+16\phi\chi)}{2976\phi\chi}, \tag{2.43}$$

$$Q_\Upsilon = -\frac{35\sqrt{\pi}(7+16\phi\chi)}{744\phi\chi}. \tag{2.44}$$

The isotropic parts $T_{ii}^{(1)}$ and $\Upsilon_{ii}^{(1)}$ are determined as follows. It can be assumed, without loss of generality, that $\Upsilon_{ii}^{(1)} = -(T_{ii}^{(1)}/\mathscr{I})$, so that the first correction to the total energy of the system, $(3(T_{ii} + \mathscr{I}\Upsilon_{ii})/2)$, is zero. The energy balance equation, which is determined by writing the conservation equation for $((c_i^2 + \mathscr{I}\omega_i^2)/2)$ in equation (2.49) below, contains the substantial derivative of the leading-order temperature ($\mathrm{D}T/\mathrm{D}t$). In order to obtain a relation for $T_{ii}^{(1)}$ as a function of the strain rate, it is necessary

to obtain an equation which does not contain the substantial derivative of the temperature. This is obtained by writing a balance equation for $(c_i^2/2 - \mathscr{I}\omega_i^2/2)$. The $O(\varepsilon)$ correction to this equation provides an expression for $T_{ii}^{(1)}$,

$$\left.\begin{aligned} T_{ii}^{(1)} &= -Q_{TI}G_{ii}, \\ \Upsilon_{ii}^{(1)} &= -Q_{\Upsilon I}G_{ii}, \end{aligned}\right\} \tag{2.45}$$

where

$$\begin{aligned} Q_{TI} = {} & \frac{\sqrt{\pi}(\mathscr{J}^2 - 8.\mathscr{I}\mathscr{J} - 32.\mathscr{I}^2 + 32\mathscr{J}.\mathscr{I}^2 - 16\mathscr{J}^2.\mathscr{I}^2)}{\mathscr{J}(-5\mathscr{J} + 40.\mathscr{I} - 16\mathscr{J}.\mathscr{I} - 288.\mathscr{I}^2 + 144\mathscr{J}.\mathscr{I}^2)} \\ & + \frac{8\sqrt{\pi}.\mathscr{I}^2}{\phi\chi\mathscr{J}(-5\mathscr{J} + 40.\mathscr{I} - 16\mathscr{J}.\mathscr{I} - 288.\mathscr{I}^2 + 144\mathscr{J}.\mathscr{I}^2)}, \end{aligned} \tag{2.46}$$

$$Q_{\Upsilon I} = -(Q_{TI}/\mathscr{I}). \tag{2.47}$$

For $\mathscr{J} = 8.\mathscr{I}/(1 + 4.\mathscr{I})$, the constant $Q_{TI}$ is given by

$$Q_{TI} = \frac{\sqrt{\pi}(1 + 4.\mathscr{I})^2(1 + 4\phi\chi)}{256.\mathscr{I}\phi\chi}. \tag{2.48}$$

The total energy balance equation is obtained by writing an equation for $(c_i^2/2 + \mathscr{I}\omega_i^2/2)$. The resulting equation is of the form

$$\rho C_v \frac{\mathrm{D}T}{\mathrm{D}t} + pG_{ii} - 2\mu S_{ik}S_{ki} - \mu_b G_{ii}^2 + RT^{3/2} = 0, \tag{2.49}$$

where $C_v$, the specific heat at constant volume, is determined to be 3, in agreement with the expectation from the equipartition of energy for a system with three translational and three rotational degrees of freedom. The dissipation function in equation (2.49), $R$, is

$$R = 4\sqrt{\pi}\varepsilon^2\rho^2\chi T^{3/2}(1 + a_t), \tag{2.50}$$

and the pressure $p$, the shear and bulk viscosities $\mu$ and $\mu_b$ are provided in equation (2.59).

The second corrections $T_{ij}^{(2)}$ and $\Upsilon_{ij}^{(2)}$ are determined from the second corrections to the balance equations for the second moments of the velocity distribution.

$$\rho\left(\frac{\mathrm{D}T_{ij}^{(1)}}{\mathrm{D}t} + T_{ik}^{(1)}G_{kj} + T_{jk}^{(1)}G_{ki}\right) = \left.\frac{\partial_c(\rho\langle c_i c_j\rangle)}{\partial t}\right|_2, \tag{2.51}$$

$$\rho\frac{\mathrm{D}\Upsilon_{ij}^{(1)}}{\mathrm{D}t} = \left.\frac{\partial_c(\rho\langle \omega_i\omega_j\rangle)}{\partial t}\right|_2. \tag{2.52}$$

The substantial derivatives on the left-hand sides of equations (2.51) and (2.52) are simplified as shown in Appendix C.

The stress $\sigma_{ij}$, which is the rate of transport, per unit area, of $i$ momentum across a surface whose unit normal is in the $j$ direction, consists of two parts. The first is the kinetic part $\sigma_{ij}^{(k)}$, which is due to the physical transport of particles along the surface, and the other is the collisional part $\sigma_{ij}^{(c)}$, which is due to the collision of particles on one side of the surface with particles on the other side,

$$\begin{aligned} \sigma_{ij}^{(k)} &= -\rho\langle c_i c_j\rangle \\ &= -\rho\left(T\delta_{ij} + \varepsilon^{1/2}T_{ij}^{(1)} + \varepsilon T_{ij}^{(2)}\right), \end{aligned} \tag{2.53}$$

$$\begin{aligned}\sigma_{ij}^{(c)} &= \tfrac{1}{2}\rho^2\chi(\phi)\int_{\boldsymbol{k}}\int_{\boldsymbol{u}}\int_{\boldsymbol{u}^*} f(\boldsymbol{x},\boldsymbol{u})f(\boldsymbol{x}^*,\boldsymbol{u}^*)(c_i'-c_i)k_j((\boldsymbol{u}-\boldsymbol{u}^*)\cdot\boldsymbol{k})\\ &= \frac{6\rho\phi\chi(\phi)}{\pi}\Bigg(\frac{-2\pi T\delta_{ij}}{3}+\frac{(8+3\mathscr{J})\sqrt{\pi T}S_{ij}}{15}+\frac{4\sqrt{\pi T}\delta_{ij}G_{kk}}{9}\\ &\quad-\frac{(4+3\mathscr{J})\pi}{15}\left(\varepsilon T_{ij}^{(1)}+\varepsilon^2 T_{ij}^{(2)}\right)+\frac{\pi\varepsilon^2\delta_{ij}}{6}\left(2+T^{-1}T_{kl}^{(1)}T_{lk}^{(1)}\right)-\frac{\pi(8+3\mathscr{J})S_{ij}G_{kk}}{90}\\ &\quad-\frac{\pi}{105}((8+3\mathscr{J})S_{ik}S_{kj}+(2-\mathscr{J})\delta_{ij}S_{kl}S_{lk})-\frac{\pi\delta_{ij}G_{kk}^2}{27}+\frac{\sqrt{\pi}\varepsilon T^{-1/2}(4+3\mathscr{J})T_{ij}^{(1)}G_{kk}}{45}\\ &\quad+\frac{\sqrt{\pi}\varepsilon T^{-1/2}}{105}\left((8+\mathscr{J})S_{ik}T_{kj}^{(1)}+8(1+\mathscr{J})T_{ik}^{(1)}S_{kj}+(4-3\mathscr{J})\delta_{ij}T_{kl}^{(1)}S_{lk}\right)\\ &\quad-\frac{1}{2\mathscr{K}\rho^2\chi}\left(A_{ik}S_{kj}+S_{ij}A_{jk}-\frac{1}{2}\left(\partial_j\left(\frac{\partial_k\sigma_{ik}}{\rho}\right)-\partial_i\left(\frac{\partial_k\sigma_{jk}}{\rho}\right)\right)\right)\Bigg),\end{aligned}\tag{2.54}$$

where $\chi$ is the pair distribution function. The total stress tensor is of the form

$$\begin{aligned}\sigma_{ij} &= -p(\phi,S_{ij},G_{ii})\delta_{ij}+2\mu(\phi,S_{ij}G_{ii})S_{ij}+\mu_b(\phi,S_{ij},G_{ii})\delta_{ij}G_{kk}\\ &\quad+\mathscr{A}_{SS}S_{ik}S_{kj}+\mathscr{A}_{SG}S_{ij}G_{kk}+\mathscr{A}_{SAS}(S_{ik}A_{kj}+S_{jk}A_{ki})\\ &\quad+\mathscr{A}_{AA}A_{ik}A_{kj}+\mathscr{A}_{SAA}(A_{ik}S_{kj}-S_{ik}A_{kj})\\ &\quad+\mathscr{C}_S\left(\frac{\partial}{\partial x_i}\left(\frac{1}{\rho}\frac{\partial p}{\partial x_j}\right)+\frac{\partial}{\partial x_j}\left(\frac{1}{\rho}\frac{\partial p}{\partial x_i}\right)-\frac{2\delta_{ij}}{3}\frac{\partial}{\partial x_k}\left(\frac{1}{\rho}\frac{\partial p}{\partial x_k}\right)\right)\\ &\quad+\frac{\delta_{ij}}{3}\left(\mathscr{B}_{SS}S_{kl}S_{lk}+\mathscr{B}_{AA}A_{kl}A_{lk}+\mathscr{B}_{GG}G_{kk}^2+\mathscr{C}_I\frac{\partial}{\partial x_k}\left(\frac{1}{\rho}\frac{\partial\sigma_{kl}}{\partial x_l}\right)\right)\\ &\quad+\mathscr{C}_A\left(\frac{\partial}{\partial x_j}\left(\frac{1}{\rho}\frac{\partial p}{\partial x_i}\right)-\frac{\partial}{\partial x_i}\left(\frac{1}{\rho}\frac{\partial p}{\partial x_j}\right)\right),\end{aligned}\tag{2.55}$$

where the pressure for rough particles is identical to that for smooth particles, and is independent of the parameters $\mathscr{I}$, $\mathscr{J}$ and $\mathscr{K}$, but the shear and bulk viscosities do depend on $\mathscr{I}$, $\mathscr{J}$ and $\mathscr{K}$,

$$p=\rho T(1+(4-2\varepsilon^2)\phi\chi),\tag{2.56}$$

$$\mu=\frac{\rho T^{1/2}Q_T}{2}+\frac{\sqrt{\pi}\rho^2\chi T^{1/2}(8+3\mathscr{J}+Q_T\sqrt{\pi}(4+3\mathscr{J}))}{30},\tag{2.57}$$

$$\mu_b=\frac{\rho T^{1/2}Q_{TI}}{3}+\rho^2\chi T^{1/2}\left(\frac{4\sqrt{\pi}}{9}+\frac{8\pi Q_{TI}}{9}\right).\tag{2.58}$$

For spherical particles $\mathscr{I}=1/10$, and in the rough limit $\mathscr{J}=8\mathscr{I}/(1+4\mathscr{I})$, the shear and bulk viscosities are

$$\left.\begin{aligned}p&=(6\phi/\pi)T(1+(4-2\varepsilon^2)\phi\chi),\\ \mu&=\frac{408T^{1/2}\phi^2\chi}{35\pi^{3/2}}+\frac{7T^{1/2}(7+16\phi\chi)^2}{992\sqrt{\pi}\chi}\\ &=T^{1/2}\left(\frac{0.195078}{\chi}+0.891784\phi+3.11265\phi^2\chi\right),\\ \mu_b&=\frac{16\phi^2T^{1/2}\chi}{\pi^{3/2}}+\frac{49T^{1/2}(1+4\phi\chi)(1+16\phi\chi)}{320\sqrt{\pi}\chi}\\ &=T^{1/2}\left(\frac{0.0863915}{\chi}+1.72783\phi+8.40245\phi^2\chi\right),\end{aligned}\right\}\tag{2.59}$$

The expression for the bulk viscosity in equation (2.59) is identical to that derived by Pidduck (1922) using the Enskog procedure in the dilute limit, but the expression for the shear viscosity shows a slight variation from that of Pidduck (1922), and the reasons for this are explained in Appendix A. The expressions for the Burnett coefficients in equation (2.55) are algebraically complicated, and so they are provided only for $\mathscr{I} = 1/10$ and in the limit $e_t \to 1$,

$$\left.\begin{aligned}
\rho^{-1}\mathscr{A}_{SS} &= -\frac{0.012873}{(\phi\chi)^2} - \frac{0.064821}{\phi\chi} - 0.544585 - 1.61492\phi\chi, \\
\rho^{-1}\mathscr{A}_{SG} &= -\frac{0.0256376}{\phi^2\chi^2} + \frac{0.152234}{\phi\chi} + 0.1292 - 1.99594\chi\phi \\
&\quad - \frac{\chi_\rho}{\chi^2}\left(0.098524 + \frac{0.043105}{\phi\chi}\right), \\
\rho^{-1}\mathscr{A}_{SAS} &= -\frac{0.020866}{\phi^2\chi^2} - \frac{0.09538}{\phi\chi} - 0.109015, \quad \rho^{-1}\mathscr{A}_{SAA} = -\frac{1}{2\mathscr{K}} = -0.1, \\
\rho^{-1}\mathscr{A}_{AA} &= \frac{0.02257}{\phi^2\chi^2} + \frac{0.103175}{\phi\chi} + 0.117914, \\
\rho^{-1}\mathscr{B}_{SS} &= -\frac{0.00057488}{\phi^2\chi^2} + \frac{0.09246}{\phi\chi} + 0.156847 - 0.88121\phi\chi, \\
\rho^{-1}\mathscr{B}_{AA} &= -\frac{0.004748}{\phi^2\chi^2} - \frac{0.002007}{\phi\chi} + 0.0900485, \\
\rho^{-1}\mathscr{B}_{GG} &= \frac{0.0031512}{\phi^2\chi^2} - \frac{0.046494}{\phi\chi} - 1.08326 - 2.84298\phi\chi \\
&\quad - \frac{\chi_\rho}{\chi^2}\left(0.0777974 + \frac{0.0340364}{\phi\chi}\right), \\
\rho^{-1}\mathscr{C}_S &= -\frac{0.0112848}{\phi^2\chi^2} - \frac{0.0515874}{\phi\chi} - 0.0589571, \\
\rho^{-1}\mathscr{C}_I &= -\frac{0.0178214}{\phi^2\chi^2} - \frac{0.11202}{\phi\chi} - 0.162938, \quad \rho^{-1}\mathscr{C}_A = -0.05.
\end{aligned}\right\} \tag{2.60}$$

The expressions for the pressure and viscosity for rough particles can be compared with the equivalent expressions for smooth particles (Kumaran 2004). The expression for the pressure is identical to that for smooth particles, and the expressions for the viscosity and the dissipation function $R$ in the energy balance equation, (2.49), are

$$\left.\begin{aligned}
\mu &= T^{1/2}\left(\frac{0.176309}{\chi} + 0.56419\phi\chi + 2.17539\phi^2\chi\right), \\
\mu_b &= 2.87339T^{1/2}\phi^2\chi, \\
R &= 4\sqrt{\pi}\varepsilon^2\rho^2\chi T^{3/2},
\end{aligned}\right\} \tag{2.61}$$

It is observed that the shear viscosity shows the same qualitative variation with density for both smooth and rough spheres, though the numerical coefficients for rough spheres are larger. This difference is small (about 10 %) in the dilute limit, but the difference is significant (about 50 %) in the dense regime. The bulk viscosity for rough spheres is, however, qualitatively different from that for smooth spheres. The bulk viscosity is zero in the dilute limit for smooth spheres, but is non-zero in the case of rough spheres. This is due to the possibility of the transport of energy

between the translational and internal (rotational) modes in the case of rough spheres, which is not present in smooth spheres. The bulk viscosity for rough spheres is also larger by a factor of about 3 than that for smooth spheres. In addition, it should be noted that the expression for smooth spheres cannot be recovered from the rough sphere calculation by taking the limit $\mathscr{I} \to 0$; a similar situation is encountered in the kinetic theories for rough elastic particles (Chapman & Cowling 1970). This is because the limit $\mathscr{I} \to 0$ is a singular limit; while there is equipartition of energy for all non-zero values of $\mathscr{I}$, there is no interchange of angular momentum between particles at $\mathscr{I} = 0$, thus preventing the equipartition of energy. All of these indicate that the stress response to volumetric compression or expansion for rough particles is significantly different from that for smooth particles, even though the response to volume preserving extensional strain may be very similar.

The expressions for the Burnett coefficients can also be compared with the equivalent expressions for smooth spheres (Kumaran 2004),

$$\left.\begin{aligned}
\rho^{-1}\mathscr{A}_{SS} &= -\frac{0.0121745}{(\phi\chi)^2} - \frac{0.0155833}{\phi\chi} - 0.242081 - 0.854446\phi\chi,\\
\rho^{-1}\mathscr{A}_{SG} &= -\frac{0.015558}{\phi^2\chi^2} - \frac{0.047615}{\phi\chi} + 0.164045 + 0.320649\chi\phi\\
&\quad - \frac{\chi_\rho}{\chi^2}\left(0.030174 + \frac{0.018856}{\phi\chi}\right),\\
\rho^{-1}\mathscr{A}_{SAS} &= -\frac{0.017044}{\phi^2\chi^2} - \frac{0.054541}{\phi\chi} - 0.043633,\\
\rho^{-1}\mathscr{A}_{SAA} &= 0,\\
\rho^{-1}\mathscr{A}_{AA} &= \frac{0.017044}{\phi^2\chi^2} + \frac{0.054541}{\phi\chi} + 0.043633,\\
\rho^{-1}\mathscr{B}_{SS} &= \frac{0.0121745}{(\phi\chi)^2} + \frac{0.0155833}{\phi\chi} + 0.242081 + 0.854446\phi\chi,\\
\rho^{-1}\mathscr{B}_{AA} &= -\frac{0.017044}{\phi^2\chi^2} - \frac{0.054541}{\phi\chi} - 0.043633,\\
\rho^{-1}\mathscr{B}_{GG} &= 0,\\
\rho^{-1}\mathscr{C}_S &= -\frac{0.0085221}{\phi^2\chi^2} - \frac{0.027271}{\phi\chi} - 0.0218166,\\
\rho^{-1}\mathscr{C}_I &= 0,\\
\rho^{-1}\mathscr{C}_A &= 0.
\end{aligned}\right\} \tag{2.62}$$

One striking difference between the Burnett coefficients for rough (equation (2.60)) and smooth (equation (2.62)) spheres is that there is an antisymmetric contribution to the stress tensor (proportional to $\mathscr{A}_{SAA}$) that is not present for smooth spheres. This contribution arises due to the substantial derivative of the mean angular velocity in equation (2.31). This indicates that the stress tensor for rough particles is not symmetric even when the mean angular velocity is equal to half the local vorticity, and there is an antisymmetric contribution due to the convective transport of angular momentum. It can easily be verified that this contribution is identically zero for a linear shear flow, but it could be non-zero for more complicated velocity profiles. There is also a significant difference in the coefficients $\mathscr{A}_{SG}$ and $\mathscr{B}_{GG}$ which multiply

the isotropic part of the rate of deformation tensor. This is consistent with the earlier finding that the bulk viscosity for rough particles is significantly different from that for smooth particles. The other coefficients are qualitatively similar for rough and smooth particles, though there are numerical differences in the values of the coefficients.

It should be noted that the antisymmetric part of the stress tensor is typically non-zero in flows of rough particles where the local angular velocity differs from half the local vorticity. In this case, micropolar theories (McCoy, Sandler & Dahler 1966; Mitarai, Hayakawa & Nakanishi 2002; Mohan, Rao & Nott 2002) assume that the antisymmetric part of the stress tensor is proportional to the difference between the local angular velocity and half the local vorticity, and the antisymmetric part of the stress tensor is identically equal to zero for a homogeneous linear shear flow where the mean angular velocity is equal to half the vorticity. In the present analysis, we predict a non-zero Burnett contribution to the antisymmetric part of the stress tensor even for a homogeneous shear flow where the mean angular velocity is half the vorticity.

### 2.2. *Partially rough particles*

For partially rough particles, the tangential coefficient of restitution $e_t$ is chosen such that $e_t = -1$ ($\mathscr{J} = 0$) for collisions in which the angle between the direction of the relative velocity and the line joining the centres of the particles is greater than $(\pi/4)$, or $\boldsymbol{k}\cdot(\boldsymbol{u}-\boldsymbol{u}^*)/|\boldsymbol{u}-\boldsymbol{u}^*| < (1/\sqrt{2})$. In this case, the relative velocity after a collision, $\boldsymbol{u}'-\boldsymbol{u}^{*\prime}$, is related to the relative velocity before a collision, $\boldsymbol{u}-\boldsymbol{u}^*$ by

$$(u_i' - u_i^{*\prime}) = (\delta_{ij} - (1+e_n)k_i k_j)(u_j - u_j^*), \tag{2.63}$$

while the angular velocities are unchanged in a collision. The tangential coefficient of restitution is close to 1 for collisions in which the angle between the line joining the centres and the direction of the relative velocity is less than $(\pi/4)$, or $(\boldsymbol{k}\cdot(\boldsymbol{u}-\boldsymbol{u}^*))/|\boldsymbol{u}-\boldsymbol{u}^*| > (1/\sqrt{2})$, and the collision rules are given by equations (2.12) and (2.13).

The analysis is carried out assuming that the leading-order velocity and angular velocity distributions are given by equations (2.19) and (2.20). The mean angular velocity and the mean square linear and angular velocities are expanded in a series in $\varepsilon$ ((2.17) and (2.18)). In the leading approximation, the equations for the mean square linear and angular velocities are

$$\left.\begin{aligned} T_{ij}^{(0)} &= T\delta_{ij}, \\ \Upsilon_{ij}^{(0)} &= \Upsilon\delta_{ij} = (T/2\mathscr{I})\delta_{ij}. \end{aligned}\right\} \tag{2.64}$$

Equation (2.64) indicates that energy is not equally partitioned between the linear and angular degrees of freedom, since not all collisions transfer momentum tangential to the contact surface. It might seem surprising that energy is not equally partitioned between the translational and rotational modes for an energy conserving collisional model in the limit where the strain rate approaches zero; however, it should be noted that a different energy conservation condition applies for different collisions. When the angle between the line of centres and relative velocity is lower than the roughness angle, the sum of the kinetic energies due to translation and rotation is conserved, whereas when the angle between the line of centres and the relative velocity is higher than the roughness angle, the kinetic energy of translation is conserved. Since only a fraction of the collisions result in interchange of energy between the translational and rotational modes, the equipartition condition is not satisfied in this case. It can also be shown that if the roughness angle is $\theta_r$, the mean square angular velocity is

given by

$$\Upsilon = \frac{(4\cos(2\theta_r) - \cos(4\theta_r) - 3)T}{4\mathscr{I}(\cos(2\theta_r) - 1)}. \tag{2.65}$$

It is easily verified that (2.65) reduces to (2.64) for roughness angle $\theta_r = (\pi/4)$, and also predicts equipartition of energy for $\theta_r = (\pi/2)$. The value of $T$ is determined from a balance between the production and dissipation of energy.

The balance equation for the angular velocity can be solved to obtain the mean angular velocity, which is, analogous to (2.31),

$$\begin{aligned}\Omega_i = &-\frac{\epsilon_{ijk}A_{jk}}{4} - \frac{\sqrt{\pi}(4-\sqrt{2})}{48}\epsilon_{ijk}A_{jk}G_{ll} + \frac{\sqrt{\pi}(4-\sqrt{2})}{80\sqrt{2}}S_{ij}\epsilon_{jkl}A_{kl} \\ &+ \frac{5\epsilon_{ijk}A_{jk}T^{(1)}_{ll}}{8} + \frac{T^{(1)}_{ij}\epsilon_{jkl}A_{kl}}{4} - \frac{3}{2\sqrt{\pi}\mathscr{J}\mathscr{K}\rho^2\chi} \\ &\times\left(\epsilon_{ijk}(A_{jl}S_{lk} + S_{jl}A_{lk}) - \frac{\epsilon_{ijk}}{2}\left(\partial_k\left(\frac{\partial_l\sigma_{jl}}{\rho}\right) - \partial_j\left(\frac{\partial_l\sigma_{kl}}{\rho}\right)\right)\right),\end{aligned} \tag{2.66}$$

where $\mathscr{K} = (1/2\mathscr{I})$, $\mathscr{J} = (4\mathscr{I}(1+e_t)/(1+4\mathscr{I}))$. It should be noted that in the leading approximation, the mean angular velocity of partially rough particles is a quarter of the vorticity, in contrast to rough particles where the mean angular velocity is half the vorticity, as indicated by equation (2.28). This is because only half the collisions result in an exchange of angular momentum between the colliding particles in the present case. This result can be generalized for other roughness angles. If $\theta_r$ is the roughness angle, the leading approximation to the mean angular velocity is given by

$$\Omega_i = -\frac{4\cos(2\theta_r) - \cos(4\theta_r) - 3}{8(\cos(2\theta_r) - 1)}\epsilon_{ijk}A_{jk}. \tag{2.67}$$

It should also be noted that there is a collisional contribution to the first correction to the mean angular velocity in equation (2.66), whereas there was no collisional contribution to the first correction in the case of rough particles in equation (2.28), and the first correction arises due to the substantial derivative in the Boltzmann equation. The equations for the pressure, viscosity and Burnett coefficients for partially rough particles were obtained in a manner similar to those for rough particles. The pressure, viscosity and the dissipation coefficient are

$$\left.\begin{aligned} p &= \rho T(1 + 4\phi\chi), \\ \mu &= T^{1/2}\left(\frac{0.195973}{\chi} + 0.712621\phi + 2.46386\phi^2\chi\right), \\ \mu_b &= T^{1/2}\left(\frac{0.159492}{\chi} + 1.12924\phi + 4.65284\phi^2\chi\right), \\ R &= 4\sqrt{\pi}\varepsilon^2\rho^2\chi T^{3/2}(1 + a_t/4). \end{aligned}\right\} \tag{2.68}$$

The expression for the pressure for partially rough spheres is identical to that for rough and smooth spheres. The shear viscosity in the dilute limit is close to that for rough spheres, but in the dense limit is significantly lower than that for rough spheres. The bulk viscosity is about half that for rough spheres in the dense limit, and about twice that for rough spheres in the dilute limit. The important conclusion is that the coefficients have the same qualitative dependence on density as those for rough spheres, though there are numerical differences. A similar conclusion applies

to the Burnett coefficients, which are given by

$$\rho^{-1}\mathscr{A}_{SS} = -\frac{0.0187355}{(\phi\chi)^2} - \frac{0.0837742}{\phi\chi} - 0.516313 - 1.27527\phi\chi, \tag{2.69a}$$

$$\rho^{-1}\mathscr{A}_{SG} = -\frac{0.0207219}{\phi^2\chi^2} - \frac{0.218434}{\phi\chi} - 2.09266 - 3.85281\chi\phi - \frac{\chi_\rho}{\chi^2}\left(0.083363 + \frac{0.044784}{\phi\chi}\right), \tag{2.69b}$$

$$\rho^{-1}\mathscr{A}_{SAS} = -\frac{0.021779}{\phi^2\chi^2} - \frac{0.079194}{\phi\chi} - 0.0719528 + 0.0132705\phi\chi, \tag{2.69c}$$

$$\rho^{-1}\mathscr{A}_{SAA} = -0.1 - 0.043575\phi\chi, \tag{2.69d}$$

$$\rho^{-1}\mathscr{A}_{AA} = \frac{0.020223}{\phi^2\chi^2} + \frac{0.066589}{\phi\chi} + 0.053879, \tag{2.69e}$$

$$\rho^{-1}\mathscr{B}_{SS} = -\frac{0.007833}{\phi^2\chi^2} + \frac{0.123102}{\phi\chi} + 0.50489 - 2.5513\phi\chi, \tag{2.69f}$$

$$\rho^{-1}\mathscr{B}_{AA} = -\frac{0.010095}{\phi^2\chi^2} - \frac{0.166484}{\phi\chi} - 0.079485, \tag{2.69g}$$

$$\rho^{-1}\mathscr{B}_{GG} = \frac{0.00038113}{\phi^2\chi^2} - \frac{0.0639626}{\phi\chi} - 0.311739 - 3.82319\phi\chi - \frac{\chi_\rho}{\chi^2}\left(0.0658254 + \frac{0.0353624}{\phi\chi}\right), \tag{2.69h}$$

$$\rho^{-1}\mathscr{C}_S = -\frac{0.010111}{\phi^2\chi^2} - \frac{0.033294}{\phi\chi} - 0.026939, \tag{2.69i}$$

$$\rho^{-1}\mathscr{C}_I = -\frac{0.010128}{\phi^2\chi^2} - \frac{0.042830}{\phi\chi} - 0.044632, \tag{2.69j}$$

$$\rho^{-1}\mathscr{C}_A = -0.05. \tag{2.69k}$$

## 3. Flow down an inclined plane

The granular material is composed of hard spherical particles flowing down a plane inclined at an angle $\theta$ to the horizontal, as shown in figure 1. A Cartesian coordinate system is used, where the velocity and velocity gradient are in the $x$ and $y$ directions, respectively, and the $z$-coordinate is in the spanwise direction. The flow is considered to be steady, fully developed and two-dimensional, so that all dynamical variables are invariant in the spanwise direction. The flow in the bulk region of the granular material is considered where the distance from the top and the bottom surface is large compared to the conduction length. In order to solve the velocity and temperature profiles, it is necessary to specify the boundary conditions for the velocity and temperature at the top and bottom surfaces. However, as explained in § 1, the rate of conduction of energy is small compared to the rate of dissipation in the bulk of the flow, and so the rate of conduction of energy can be neglected in the bulk in the leading approximation. The temperature in the bulk is determined from the balance between the rates of production and dissipation, while the temperature boundary condition only affects the temperature in the conduction regions near the boundaries. It is necessary to specify the velocity boundary conditions in order to determine the complete velocity profile, since momentum is a conserved variable. However, it should be noted that only the strain rate is calculated from the stress

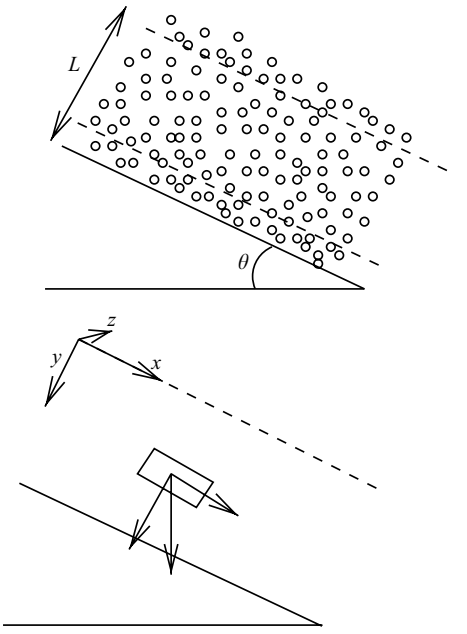


FIGURE 1. Configuration and coordinate system used for analysing the flow down an inclined plane.

balance conditions in the present analysis. The velocity is determined by integrating the strain rate with respect to the $y$ coordinate, and the velocity boundary condition at the bottom can be used to determine the constant in the integration.

The normal and shear stresses balance the gravitational forces in the flow and gradient directions,

$$(\mathrm{d}\sigma_{xy}/\mathrm{d}y) = \rho g \sin(\theta), \;\; (\mathrm{d}\sigma_{yy}/\mathrm{d}y) = -\rho g \cos(\theta). \tag{3.1}$$

The ratio of the shear and normal stresses is a constant in the flow,

$$(\sigma_{xy}/\sigma_{yy}) = -\tan(\theta). \tag{3.2}$$

Equation (3.2) relating the shear and normal stress provides the relation between the angle of inclination and the volume fraction, as explained following equation (3.5).

The ratio of the shear and normal stresses are analysed for the three constitutive models used here, the smooth particle model (equations (2.61) and (2.62)), the rough particle model (equations (2.59) and (2.60)), and the partially rough particle model (equations (2.68) and (2.69)). The 'temperature' $T$ is determined, in terms of the strain rate, from a balance between the source of energy due to the mean shear, and the dissipation due to inelastic collisions,

$$\mu\dot{\gamma}^2 = RT^{3/2}, \tag{3.3}$$

where $R$, given in equations (2.59), (2.61) and (2.68), is only a function of the volume fraction of the particles and the coefficients of restitution. The energy balance can be solved to obtain the strain rate,

$$\dot{\gamma} = T^{3/4}(R/\mu)^{1/2}. \tag{3.4}$$

It can be inferred, from the temperature dependences of the viscosity and the normal stress, that the volume fraction is independent of the $y$-coordinate in the flow.

Equation (3.2) relating the shear and normal stress, together with equation (2.55) for the shear and normal stresses, gives

$$\frac{\sqrt{R\mu T^{3/2}}}{\left(p+\left(T^{3/2}R/\mu\right)(3(\mathscr{A}_{AA}-\mathscr{A}_{SS})+6\mathscr{A}_{SAS}+2(\mathscr{B}_{AA}-\mathscr{B}_{SS}))/12\right)}=\tan\theta. \tag{3.5}$$

In equation (3.5), the numerator is proportional to $T$, since the viscosity $\mu$ is proportional to $T^{1/2}$. In the denominator, both the pressure and the Burnett contributions to the stress are proportional to $T$. Therefore, the left-hand side of the equation is independent of $T$, and is dependent only on the volume fraction $\phi$ and the coefficient of restitution. The right-hand side is a constant independent of $\phi$, and so equation (3.5) implies that $\phi$ is independent of position if the left-hand side is a monotonic function of $\phi$. This result is also applicable to more general forms of the constitutive relations for the granular flow, if there is a balance between the local rate of production of energy due to mean shear and the rate of dissipation due to inelastic collisions. Since the inverse of the local strain rate provides the only time scale in the problem, the temperature has to scale as the square of the strain rate, and the stress has to scale as the square of the strain rate. Therefore, the volume fraction is independent of position, and is only a function of the angle of inclination. The invariance of the density in the cross-stream direction is observed in the simulations of Silbert *et al.* (2001) when the height of the flow is greater than about 10 particle diameters, though it is not applicable to very thin flows because the length scale is not large compared to the conduction length and the adiabatic approximation is not valid. The other flow parameters, such as the strain rate, temperature and the velocity profile are determined from the value of the density as described a little later.

It might be intuitively expected that the volume fraction decreases as the angle of inclination is increased, and the volume fraction is equal to the volume fraction at close packing at the cessation of flow. Though this requirement seems fairly basic, not all microscopic models satisfy this requirement, as shown a little later. The variation of volume fraction with angle of inclination is first examined in the limits of low density and near close packing, in order to examine whether the angle of inclination is a decreasing function of density in these limits. Another reason for examining these cases is that the results turn out to be independent of the form of the pair distribution function. The intermediate regime is next considered, using two different forms of the pair distribution function used previously in literature. The Carnahan–Starling pair distribution function, which is a good model at low and moderate volume fractions, is

$$\chi(\phi)=\frac{2-\phi}{2(1-\phi)^3}, \tag{3.6}$$

and the high density pair distribution function, which is a good model as the close packing volume fraction is approached, is

$$\chi(\phi)=\frac{1}{1-(\phi/\phi_c)^{1/3}}, \tag{3.7}$$

where $\phi_c$, the volume fraction at close packing, is set equal to 0.65 in the results presented here.

It should be noted that the criterion for the onset of flow as the angle of inclination is increased could be different from the criterion for the cessation of flow as the angle of inclination is decreased. As the angle of inclination is increased for a static granular layer, the angle of inclination for the onset of flow is determined by the static yield

condition, which depends, in general, on the conditions under which this layer was prepared. The angle at which flow stops as the angle of inclination of a flowing layer is decreased is the minimum angle required to sustain flow in equation (3.2), which is the ratio of the shear and normal stress in the close packing limit. The minimum angle calculated here is the angle at which there is cessation of flow when the angle of inclination of a flowing layer is reduced. If the static angle of friction is larger than the minimum angle required to sustain flow, then there will be a discontinuous change in density at the onset of flow. The implications of the opposite case, where the static angle of friction is smaller than the minimum flow angle, are not clear. It is possible that the flow will be confined to a thin region at the bottom of the granular layer, while the rest flows as a plug.

In the limit of small volume fraction, the left-hand side of equation (3.2) can be expanded in a series in the volume fraction,

$$A_0 + A_1\phi\chi + A_2\phi^2\chi^2 = \tan(\theta), \tag{3.8}$$

where the functions $A_0$, $A_1$ and $A_2$ are given by

$$\left.\begin{aligned} A_0 &= \frac{1.2522\varepsilon}{1.12-\varepsilon^2}, \\ A_1 &= \frac{-1.2022\varepsilon(2.8-\varepsilon^2)}{(1.12-\varepsilon^2)^2}, \\ A_2 &= \frac{26.342\varepsilon(\varepsilon^4-1.781\varepsilon^2+0.8639)}{(1.12-\varepsilon^2)^3}, \end{aligned}\right\} \tag{3.9}$$

for smooth particles,

$$\left.\begin{aligned} A_0 &= \frac{3.91086\varepsilon_r}{3.32545-\varepsilon_r^2}, \\ A_1 &= \frac{-10.1499\varepsilon_r\left(2.1976-2.56383\varepsilon^2-\varepsilon_r^2\right)}{\left(3.32545-\varepsilon_r^2\right)^2}, \\ A_2 &= \frac{392.511\varepsilon_r(\varepsilon_r^4-3.7048\varepsilon_r^2+0.495269\varepsilon^2\varepsilon_r^2+0.440739\varepsilon^4-1.25925\varepsilon^2+1.34678)}{\left(3.32545-\varepsilon_r^2\right)^3}, \end{aligned}\right\} \tag{3.10}$$

for rough particles, and

$$\left.\begin{aligned} A_0 &= \frac{5.85124\varepsilon_{pr}}{4.964-\varepsilon_{pr}^2}, \\ A_1 &= \frac{-160.763\varepsilon_{pr}\left(0.39411-\varepsilon_{pr}^2-0.361345\varepsilon^2\right)}{\left(4.964-\varepsilon_{pr}^2\right)^2}, \\ A_2 &= \frac{5468.4\varepsilon_{pr}\left(\varepsilon_{pr}^4-1.6392\varepsilon_{pr}^2+0.603063\varepsilon^2\varepsilon_{pr}^2+0.105466\varepsilon^4-0.325986\varepsilon^2+0.352274\right)}{\left(4.496-\varepsilon_{pr}^2\right)^3}, \end{aligned}\right\} \tag{3.11}$$

for partially rough particles in the Burnett approximation, where $\varepsilon_r = \varepsilon(1+a_t)^{1/2}$, and $\varepsilon_{pr} = \varepsilon(1+a_t/4)^{1/2}$. The Navier–Stokes results for equations (3.9), (3.10) and (3.11) are obtained by retaining only the terms proportional to $\varepsilon$ in the limit $\varepsilon \to 0$. These results

indicate that the maximum angle for steady flow increases proportional to $\varepsilon$. Another qualitative feature of the flow curve is the slope in the limit of low density, which is given by $A_1$. If the slope is negative, the angle of inclination decreases as the density increases, indicating that the angle of inclination is a maximum in the limit of zero density. If the slope is positive, the angle of inclination increases as density increases, and the maximum angle of inclination corresponds to a flow with finite density. It is observed that $A_1$ is always negative for smooth particles, indicating that the maximum angle of inclination corresponds to the limit of zero density. For rough particles, $A_1$ is positive for $\varepsilon_r^2 + 2.56383\varepsilon^2 > 2.1976$, which is equivalent to $e_n < 0.518475$ for $a_t = 1$. However, it should be noted that the asymptotic analysis requires $(1 - e_n) \ll 1$, and $A_1$ is negative in this limit for rough particles. In the case of partially rough particles, $A_1$ is positive for $\varepsilon_{pr}^2 + 0.361345\varepsilon^2 - 0.39411 > 0$, which is equivalent to $e_n < 0.755416$ for $a_t = 1$. Clearly, $A_1$ is positive for a larger range of coefficients of restitution for the partially rough sphere model.

When the volume fraction is near close packing, the left-hand side of (3.2) can be expanded in a series in the inverse of the pair distribution function, since the pair distribution function diverges near close packing. This results in an expression of the form

$$B_0 + B_1(\phi\chi)^{-1} + B_2(\phi\chi)^{-2} = \tan(\theta). \tag{3.12}$$

The above expansion shows that there is dilation upon initiation of flow only if $B_1 > 0$. If $B_1 < 0$, the flow becomes more dense as the angle of inclination is increased, in contrast to the normally expected dilation upon commencement of flow. Densification is a possibility when flow starts, if the volume fraction in the stationary state is lower than the packing fraction at random close packing, but we do not examine this further since it does not seem to have been seen in experiments or simulations, and restrict attention to flows where $B_1$ is positive.

In the Burnett approximation, the coefficients in equation (3.12) are

$$\left.\begin{aligned} B_0 &= \frac{3.40449\varepsilon}{(3.46757 - \varepsilon^2)}, \\ B_1 &= -\frac{0.136503\varepsilon(10.4061 - \varepsilon^2)}{(3.46757 - \varepsilon^2)^2}, \\ B_2 &= \frac{0.671819\varepsilon(\varepsilon^4 - 2.48775\varepsilon^2 - 3.78982)}{(3.46757 - \varepsilon^2)^3}, \end{aligned}\right\} \tag{3.13}$$

for smooth spheres,

$$\left.\begin{aligned} B_0 &= \frac{1.02693\varepsilon_r}{\left(0.874417 + \varepsilon_r^2 - 0.437208\varepsilon^2\right)}, \\ B_1 &= -\frac{0.254845\varepsilon_r\left(0.376137 + 0.252379\varepsilon^2 - \varepsilon_r^2\right)}{\left(0.874417 + \varepsilon_r^2 - 0.437208\varepsilon^2\right)^2}, \\ B_2 &= \frac{0.121859\varepsilon_r\left(\varepsilon_r^4 + 0.298183\varepsilon_r^2 + 0.307759 - 0.4743089\varepsilon_r^2\varepsilon^2 + 0.033950\varepsilon^4 - 0.020421\varepsilon^2\right)}{\left(0.874417 + \varepsilon_r^2 - 0.437208\varepsilon^2\right)^3}, \end{aligned}\right\} \tag{3.14}$$

for rough spheres, and

$$\left.\begin{aligned} B_0 &= \frac{0.530463\varepsilon_{pr}}{\left(0.50768+\varepsilon_{pr}^2-0.25384\varepsilon^2\right)},\\ B_1 &= \frac{0.223654\varepsilon_{pr}\left(\varepsilon_{pr}^2-0.087067\varepsilon^2-0.126896\right)}{\left(0.50768+\varepsilon_{pr}^2-0.25384\varepsilon^2\right)^2},\\ B_2 &= \frac{0.11272\varepsilon_{pr}\left(\varepsilon_{pr}^4-0.022895\varepsilon_{pr}^2-0.197195\varepsilon_{pr}^2\varepsilon^2-0.013628\varepsilon^2+0.00889\varepsilon^4+0.067511\right)}{\left(0.50768+\varepsilon_{pr}^2-0.25384\varepsilon^2\right)^3}, \end{aligned}\right\} \tag{3.15}$$

for partially rough spheres. The results in the Navier–Stokes approximation are obtained by truncating the above equations at $O(\varepsilon)$. Clearly, the coefficient $B_1$ is negative in all cases in the Navier–Stokes approximation, resulting in an increase in density as the angle of inclination is increased near close packing in the Navier–Stokes approximation. In the case of smooth nearly elastic spheres, it is observed that $B_1$ is positive only for $\varepsilon^2=(1-e_n)>10.4061$ in the Burnett approximation. This is clearly not realizable, because the coefficient of restitution is always less than 1, and so the Burnett approximation for smooth nearly elastic spheres also predicts that the granular material becomes more dense as the angle of inclination is increased. For rough nearly elastic spheres, $B_1$ is positive for $\varepsilon_r^2-0.252379\varepsilon^2>0.376137$. This is physically realizable; for example, for $a_t=1$, the coefficient $B_1$ is positive for $e_n<0.784472$. For partially rough spheres, $B_1$ is positive for $(1+a_t/4)\varepsilon^2-0.087067\varepsilon^2>0.126896$, which is equivalent to $e_n<0.89088$ for $a_t=1$. Therefore, the rough and partially rough sphere models provide realistic results for the dependence of density on the angle of inclination over a range of coefficients of restitution in the dense limit. The values of $\varepsilon$ at which $B_1$ becomes positive, which is 0.46 for the rough sphere model and 0.33 for the partially rough particle model, are not small compared to 1. However, it should be noted that the error in the constitutive relations due to the neglect of higher-order terms in the $\varepsilon$ expansion is still small for these values of $\varepsilon$. The constitutive relations are obtained correct to $O(\varepsilon^2)$, and the error in the constitutive relation is $O(\varepsilon^3)$ which is about 10 % at $\varepsilon=0.46$, and about 3.6 % at $\varepsilon=0.33$.

The dependence of the angle of inclination on the density in the intermediate regime in the Navier–Stokes approximation is shown in figure 2 for two different forms of the pair correlation function. Since $\tan(\theta)\propto\varepsilon$ in the limit $\varepsilon\to0$, figure 2 shows $(\tan(\theta)/\varepsilon)$ for smooth spheres, $(\tan(\theta)/\varepsilon(1+a_t)^{1/2})$ for rough spheres and $(\tan(\theta)/\varepsilon(1+a_t/4)^{1/2})$ for partially rough spheres. The curves have a qualitatively similar behaviour for both the Carnahan–Starling and the high-density pair distribution functions. Both models for the pair distribution provide results identical to (3.9), (3.10) and (3.11) in the low-density limit. The high-density pair distribution function provides accurate results near close packing, since it diverges in this limit. The Carnahan–Starling pair distribution is not expected to provide exact results in this limit, since it does not diverge, but the results are numerically close to those predicted by equations (3.13), (3.15) and (3.14). In all cases, it is observed that the angle of inclination first decreases as the density is increased, reaches a minimum and then increases as the density is further increased. The slope in the high-density limit is always positive, indicating that the density increases as the angle of inclination is increased. The physical implication of this is as follows. The minimum angle at which steady flow can be sustained corresponds to the minimum of the curves in figure 2, which occurs at around $\phi=0.2$. This indicates

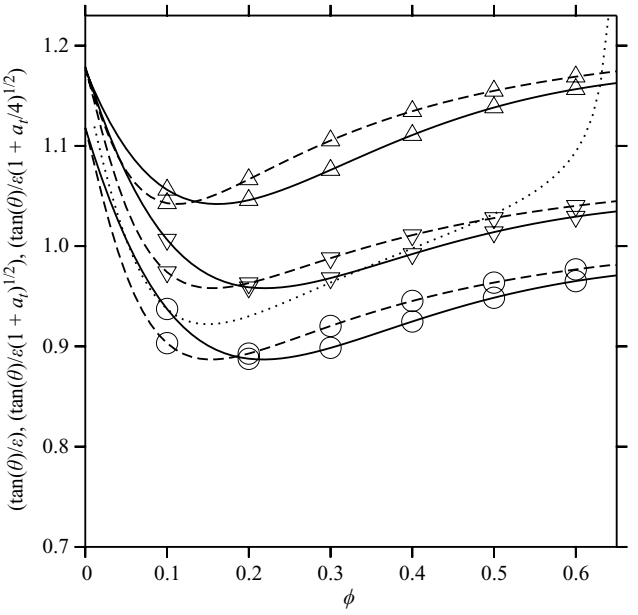


FIGURE 2. Variation of $(\tan(\theta)/\varepsilon)$ for smooth spheres ($\bigcirc$), $(\tan(\theta)/\varepsilon(1+a_t)^{1/2})$, for rough spheres ($\triangle$) and $(\tan(\theta)/\varepsilon(1+a_t/4)^{1/2})$ for partially rough spheres ($\triangledown$) as a function of density $\phi$ for the Carnahan–Starling pair distribution function equation (3.6) (solid line) and the high-density pair distribution function (3.7) (broken line). The dotted line shows the results for smooth particles when the pair distribution function is given by the high-density pair distribution (3.7), and the viscosity is modified as shown in equation (3.30). Here, $\theta$ is the angle of inclination from the horizontal, $\varepsilon = \sqrt{1-e_n}$, and $a_t = (1-e_t^2)/(1-e_n^2)$.

that as the angle of inclination is decreased, there is a discontinuous change in density from 0.2 to the close packing density for a static assembly of particles when flow stops. In addition, as the angle of inclination is increased from this minimum value, there are two possible steady states, one corresponding to densification and the other to a decrease in the density as the angle of inclination is increased. This seems to be at variance with most experimental and simulation studies, which indicate that the density is near close packing just before flow cessation, and one is forced to conclude that the Navier–Stokes approximation does not provide accurate results for the dependence of density on the angle of inclination.

Next, the flow curves are examined in the Burnett approximation over a range of values of $\varepsilon$, and attention is restricted to the case $a_t = 1$ for rough and partially rough particles for definiteness. Figure 3 shows the results for smooth particles. It is observed that the angle of inclination exhibits a minimum at intermediate density as $\varepsilon$ is increased, but the value of the minimum is close to the value of the density at close packing. This angle of inclination is nearly a constant as density is increased beyond about 0.2 for $\varepsilon^2 > 0.3$, indicating that a large variation in density could be caused by a small variation in the angle of inclination. However, the angle of inclination always increases with density near close packing in all cases. The results for the Carnahan–Starling and the high-density pair distribution functions are in agreement for $\phi > 0.3$, though there is some disagreement at low densities where the high-density pair distribution function is not expected to be accurate. The results for rough particles are shown in figure 4, and it is observed that the angle of inclination is a decreasing function of density near close packing for $\varepsilon^2 = 0.4$ and 0.5. In addition,

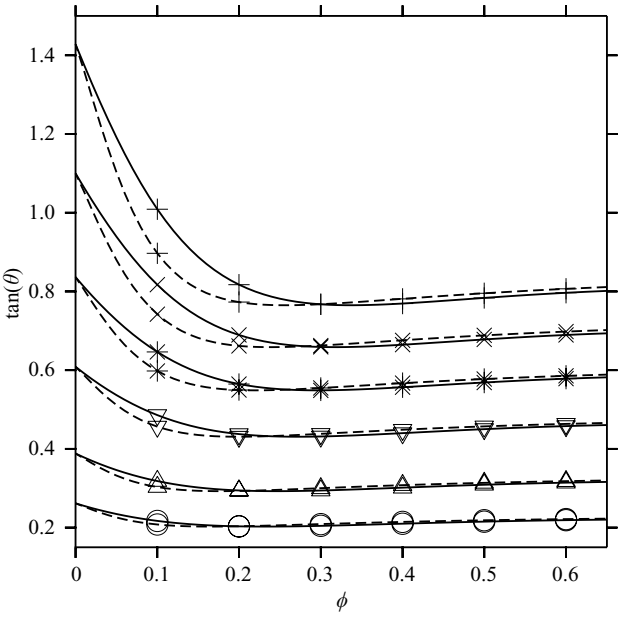


FIGURE 3. Variation of $\tan(\theta)$ for smooth spheres as a function of density $\phi$ for $\varepsilon^2 = 0.05$ ($\circ$), $\varepsilon^2 = 0.1$ ($\triangle$), $\varepsilon^2 = 0.2$ ($\nabla$), $\varepsilon^2 = 0.3$ ($*$), $\varepsilon^2 = 0.4$ ($\times$), $\varepsilon^2 = 0.5$ ($+$) for the Carnahan–Starling pair distribution function equation (3.6) (solid line) and the high-density pair distribution function (3.7) (broken line). Here, $\theta$ is the angle of inclination from the horizontal, $\varepsilon = \sqrt{1 - e_n}$.

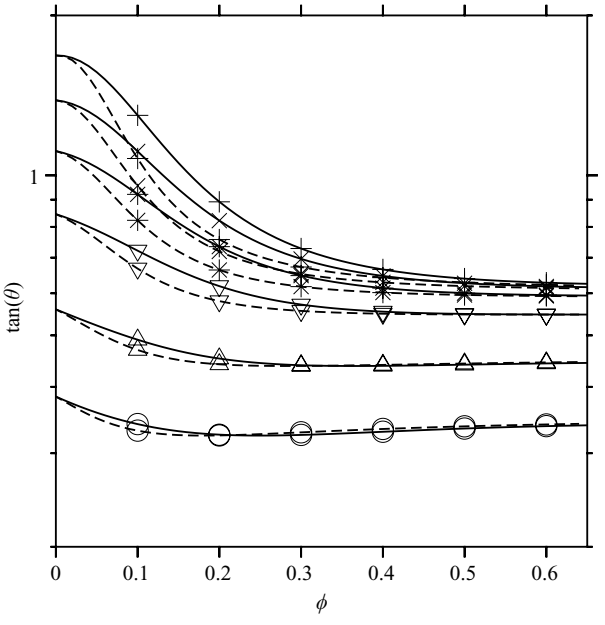


FIGURE 4. Variation of $\tan(\theta)$ for rough spheres as a function of density $\phi$ for $a_t = 1$ and $\varepsilon^2 = 0.05$ ($\circ$), $\varepsilon^2 = 0.1$ ($\triangle$), $\varepsilon^2 = 0.2$ ($\nabla$), $\varepsilon^2 = 0.3$ ($*$), $\varepsilon^2 = 0.4$ ($\times$), $\varepsilon^2 = 0.5$ ($+$) for the Carnahan–Starling pair distribution function equation (3.6) (solid line) and the high-density pair distribution function (3.7) (broken line). Here, $\theta$ is the angle of inclination from the horizontal, $\varepsilon = \sqrt{1 - e_n}$, and $a_t = (1 - e_t^2)/(1 - e_n^2)$.

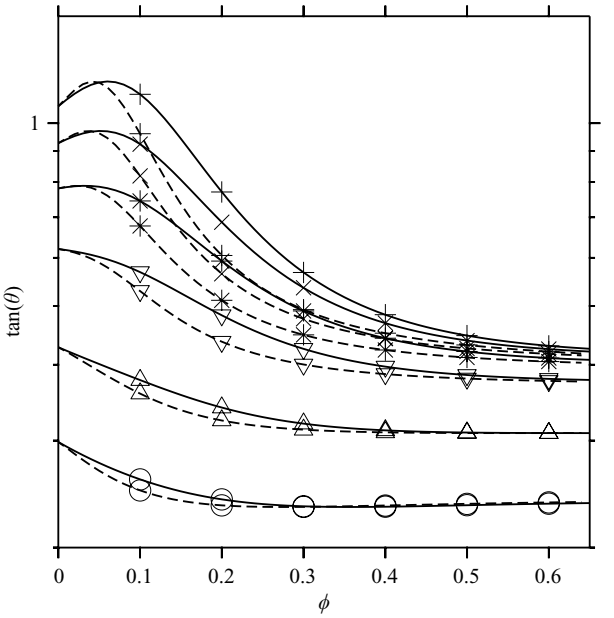


FIGURE 5. As figure 4, but for partially rough spheres.

the angle of inclination does not show significant variation with the parameter $\varepsilon^2$ when $\varepsilon^2$ increases beyond about 0.3 near close packing, though there is significant variation in the low-density limit. The results for partially rough particles, shown in figure 5, indicate that the angle of inclination is a decreasing function of density over a much larger range $\varepsilon^2 = 0.2$ and higher. In addition, the angle of inclination is not very sensitive to the parameter $\varepsilon^2$ when this parameter increases beyond 0.2. Another feature of interest is the slight increase in the angle of inclination with density in the limit of low density for $\varepsilon^2 = 0.4$ and $\varepsilon^2 = 0.5$, as anticipated from equation (3.11).

It is of interest to examine the variation of the angles of inclination in the low-density limit, $\theta_l$, and near close packing, $\theta_c$, with the coefficients of restitution. In addition, if $\theta$ is not a monotonic function of $\phi$, the maximum angle of inclination $\theta_{max}$, could be different from the angle of inclination in the limit of low density (as in the case of partially rough particles in figure 5), and the minimum angle of inclination, $\theta_{min}$ could be different from that in the limit of close packing (as in the case of smooth particles in figure 3). Thus, there are four important angles of inclination, the angle in the low-density limit $\theta_l$, the maximum angle $\theta_{max}$ at which a steady flow can be sustained, the angle in the close packing limit $\theta_c$, and the minimum angle for flow $\theta_{min}$. These angles are shown as a function of $\varepsilon^2$ for smooth particles in figure 6. All of these angles increase proportional to $\varepsilon$ in the limit $\varepsilon \to 0$, as expected from the Navier–Stokes approximation. It is observed that $\tan(\theta_{min})$ is always slightly lower than $\tan(\theta_c)$, indicating that there is densification with an increase in the angle of inclination in the dense limit, though the difference between $\theta_{min}$ and $\theta_c$ is small. However, both $\theta_c$ and $\theta_{min}$ increase as $\varepsilon^2$ is increased in the dilute limit. A similar graph for rough particles is shown in figure 7. It is observed that $\theta_{min}$ is lower than $\theta_c$ only for $\varepsilon^2 < 0.192$ for $a_t = 1$, as expected from equation (3.14), while the minimum of the angle of inclination occurs at close packing for $\varepsilon^2 > 0.192$. In addition, it is observed that $\theta_c$, the minimum angle for flow, is relatively insensitive to variations in $\varepsilon^2$, and it varies from 25.6° at $\varepsilon^2 = 0.3$ to 28.7° at $\varepsilon^2 = 0.8$. However, there is a

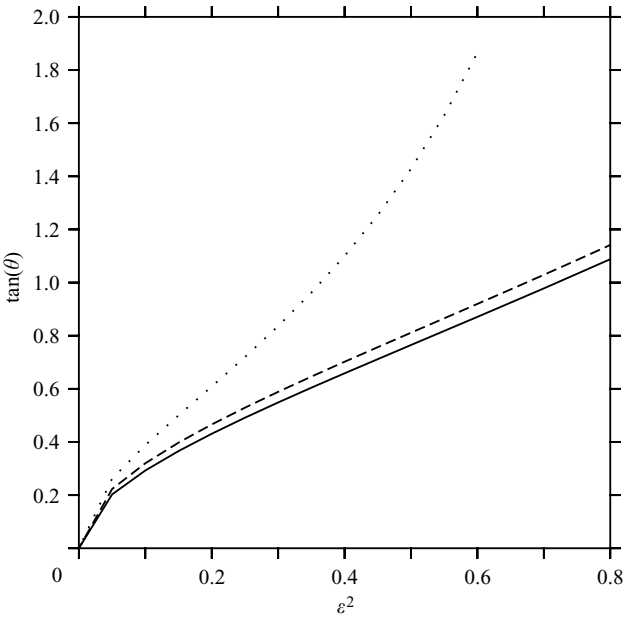


FIGURE 6. Variation of $\tan(\theta_l)$ (dotted line), $\tan(\theta_c)$ (dashed line) and $\tan(\theta_{min})$ (solid line) with $\varepsilon^2$ for smooth particles. Here, $\theta$ is the angle of inclination from the horizontal, $\varepsilon = \sqrt{1-e_n}$.

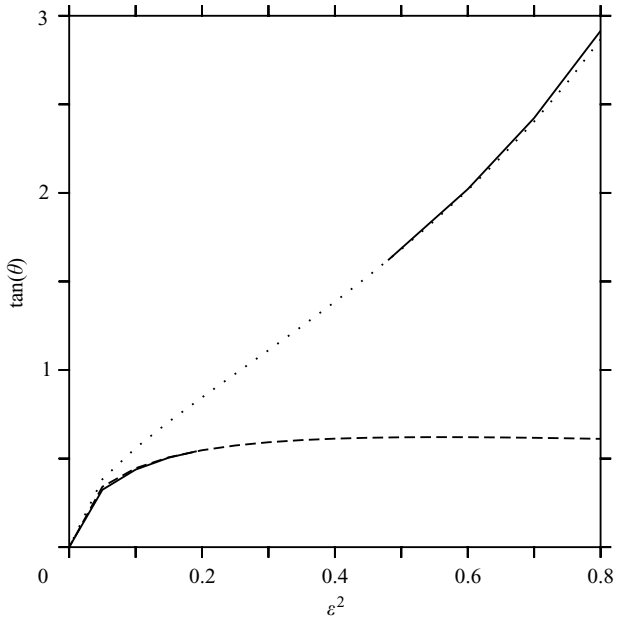


FIGURE 7. Variation of $\tan(\theta_l)$ (dotted line), $\tan(\theta_c)$ (dashed line) and $\tan(\theta_{min})$ (lower solid line) and $\tan(\theta_{max})$ (upper solid line) with $\varepsilon^2$ for $a_t = 1$ for rough particles. Here, $\theta$ is the angle of inclination from the horizontal, $\varepsilon = \sqrt{1-e_n}$, and $a_t = (1-e_t^2)/(1-e_n^2)$.

significant variation of $\theta_l$ with $\varepsilon^2$. In addition, $\theta_{max}$ is higher than $\theta_l$ for $\varepsilon^2 > 0.48$. The qualitative behaviour is similar for partially rough particles, as shown in figure 8, though $\theta_c$ is lower than $\theta_{min}$ onlyfor a much smaller range $\varepsilon^2 < 0.099$ at $a_t = 1$, and

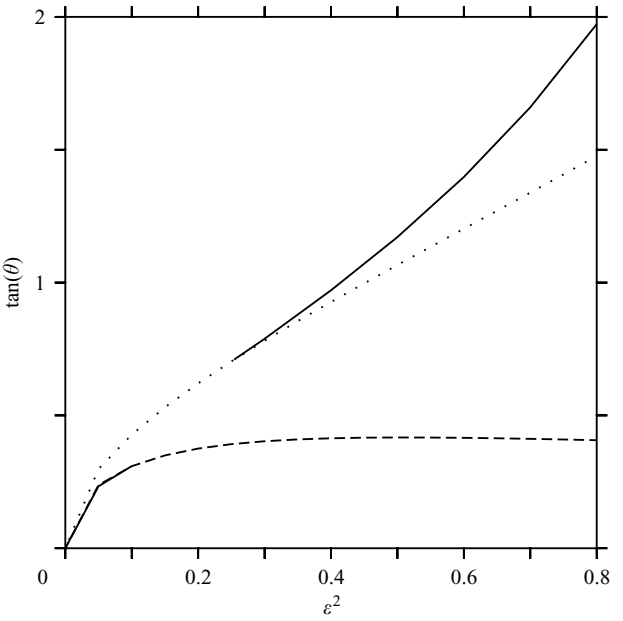


FIGURE 8. As figure 7, but for partially rough particles.

the minimum angle of inclination is at close packing for $\varepsilon^2 > 0.099$. The variation of $\theta_c$ with $\varepsilon^2$ in this case is smaller than that for rough spheres, and $\theta_c$ varies from $19.79^\circ$ at $\varepsilon^2 = 0.3$ to $19.38^\circ$ at $\varepsilon^2 = 0.8$. The maximum angle $\theta_{max}$ is higher than $\theta_l$ over a larger range $\varepsilon^2 > 0.256$ in this case.

To summarize the results so far, starting from the condition that the ratio of the tangential and normal stresses is equal to $\tan(\theta)$, it was shown following equation (3.5) that the volume fraction of the particles is a constant across the flow. The value of this constant was then evaluated using equations (2.59)–(2.62), (2.68) and (2.69) for the different particle models. It was found that if the Burnett terms were not included in the constitutive relation, there was densification when the angle of inclination was increased for all particle models. A similar result was encountered for smooth nearly elastic particles when the Burnett terms were included in the stress tensor. However, when the Burnett terms were included in the stress tensor for rough and partially rough particles, it was found that the volume fraction decreased as the angle of inclination increased over a range of tangential and normal coefficients of restitution. This indicates that the numerical value of the volume fraction is sensitive to the model used for the stress tensor and for particle collisions.

One of the striking features of the simulations of Silbert *et al.* (2001) is that the density profile at a fixed angle of inclination is remarkably insensitive to changes in the coefficients of restitution. This feature is also observed in the present analysis for rough and partially rough particles, where the variation of the angle of inclination near close packing is insensitive to the parameter $\varepsilon^2$ over a significant range in the Burnett approximation in figures 7 and 8, though the same trend is not observed in the Navier–Stokes approximation. This indicates that the Burnett approximation for the stress does capture the lack of sensitivity $\theta_c$ to variations in the coefficients of restitution over a range of values of $\varepsilon$.

The first normal stress difference for the constitutive relation equation (2.55) is

$$\sigma_{xx} - \sigma_{yy} = -\mathscr{A}_{SAS}\dot{\gamma}^2. \tag{3.16}$$

where $\dot{\gamma} = (\mathrm{d}u_x/\mathrm{d}y)$ is the mean strain rate. Equations (2.60), (2.62) and (2.69) provide the following predictions for the first normal stress difference,

$$\sigma_{xx} - \sigma_{yy} = \left(\frac{0.0325727}{\phi\chi^2} + \frac{0.104166}{\chi} + 0.083333\phi\right)\dot{\gamma}^2 \tag{3.17}$$

for smooth particles,

$$\sigma_{xx} - \sigma_{yy} = \left(\frac{0.0398514}{\phi\chi^2} + \frac{0.182178}{\chi} + 0.208203\phi\right)\dot{\gamma}^2 \tag{3.18}$$

for rough particles, and

$$\sigma_{xx} - \sigma_{yy} = \left(\frac{0.0415941}{\phi\chi^2} + \frac{0.151249}{\chi} + 0.13742\phi - 0.0253447\phi^2\chi\right)\dot{\gamma}^2 \tag{3.19}$$

for partially rough particles. The first normal stress difference is found to be positive for smooth and rough particles, and is found to approach a finite value in the limit of close packing. However, for partially rough particles, the normal stress difference is negative and diverges proportional to $\chi$ in the close packing limit, but becomes negative as the volume fraction is increased. In addition, it is found that the coefficient of the $\phi^2\chi$ term in equation (3.19) is small, indicating that the transition from positive to negative values of the normal stress difference takes place at $\phi = 0.598$ for the Carnahan–Starling pair distribution function 3.6 and $\phi = 0.508$ for the high-density pair distribution function (3.7), both of which are near close packing. This sensitivity of the normal stress difference to the choice of model was also encountered in the simulations of Silbert *et al.* (2001), where it was observed that the normal stress difference is always positive for some of the particle models used, but underwent a transition from positive values very near close packing to negative values as the density is decreased for other particle models. (It should be noted that the sign convention used for the stress in Silbert *et al.* (2001) is opposite to that used here, and the leading contribution to the normal stress is equal to the negative of the pressure in the present analysis, whereas it is equal to the pressure in the sign convention used by Silbert *et al.*) In addition, it is also found that the value of the first normal stress difference is small compared to the value of the normal stress itself. For example, in the dense limit, the ratio $(\sigma_{xx} - \sigma_{yy})/p$ is $(0.226429(1 + a_t)\varepsilon^2/(\phi\chi))$ in the limit of close packing for the rough particle model, and $(-0.032419 + 0.193796/(\phi\chi))(1 + a_t/4)\varepsilon^2$ for the partially rough particle model. The small relative magnitude of the first normal stress difference was also reported by Silbert *et al.* (2001).

The second normal stress difference, $\sigma_{yy} - \sigma_{zz}$, is given by

$$\sigma_{yy} - \sigma_{zz} = \left(-\frac{\mathscr{A}_{AA}}{4} + \frac{\mathscr{A}_{SAS}}{2} + \frac{\mathscr{A}_{SS}}{4}\right)\dot{\gamma}^2 \tag{3.20}$$

Equations (2.60), (2.62) and (2.69) provide the following predictions for the first normal stress difference,

$$\sigma_{yy} - \sigma_{zz} = \left(-\frac{0.112131}{\chi} - \frac{0.033139}{\chi^2\phi} - 0.310213\phi - 0.420131\chi\phi^2\right)\dot{\gamma}^2 \tag{3.21}$$

for the smooth particle model,

$$\sigma_{yy} - \sigma_{zz} = \left( -\frac{0.171301}{\chi} - \frac{0.0368475}{\chi^2 \phi} - 0.420422\phi - 0.771067\chi\phi^2 \right) \dot{\gamma}^2 \qquad (3.22)$$

for the rough particle model, and

$$\sigma_{yy} - \sigma_{zz} = \left( -\frac{0.147418}{\chi} - \frac{0.0393984}{\chi^2 \phi} - 0.340957\phi - 0.596222\chi\phi^2 \right) \dot{\gamma}^2 \qquad (3.23)$$

for the partially rough particle model. Note that the second normal stress difference is negative, in agreement with the observations of Silbert *et al.* (2001). It is also observed that the second normal stress difference is significantly larger in magnitude than the first normal stress difference for the rough and partially rough particle models, and is negative in all cases. The ratio $(\sigma_{yy} - \sigma_{zz})/p$ is $-0.838466(1 + a_t)\varepsilon^2$ for the rough particle model in the dense limit, and $-0.762656(1 + a_t/4)\varepsilon^2$ for the partially rough particle model. Silbert *et al.* (2001) reported that this ratio was about 15 % in the simulations, which is consistent with our results for $a_t = 1$ at $e_n = 0.9$ for the rough particle model, and $e_n = 0.84$ for the partially rough particle model.

The dependence of the volume fraction on the angle of inclination near close packing can be determined as follows. If we only retain the terms proportional to $B_0$ and $B_1$ in the expansion (3.12), we obtain

$$\phi\chi(\phi) = B_1(\tan(\theta) - \tan(\theta_0))^{-1} \approx B_1\left(B_0^2 + 1\right)^{-1}(\theta - \theta_0)^{-1} \qquad (3.24)$$

when the angle $\theta$ is close to $\theta_0$. Thus, $\phi\chi(\phi)$ diverges proportional to $(\theta - \theta_0)^{-1}$ when the angle of inclination is close to $\theta_0$, and the dependence of the density on the angle of inclination depends on the model used for the pair distribution function. The high-density pair distribution function (3.7) diverges as $\chi'(\phi_c - \phi)^{-1}$ in the close packing limit limit $\phi \to \phi_c$.

$$(\phi_c - \phi) = \left(B_0^2 + 1\right)\chi'\phi_c(\theta - \theta_0)/B_1. \qquad (3.25)$$

This linear dependence of the volume fraction on the angle of inclination is in agreement with the simulation results of Silbert *et al.* (2001).

The flow dynamics can be described using the 'Bagnold law' for the shear stress,

$$\sigma_{xy} = A_B^2\dot{\gamma}^2. \qquad (3.26)$$

Since the tangential stress is given by $\rho g(h - y)\sin(\theta)$, equation (3.26) gives the strain rate as a function of height once $A_B$ is known (note that $A_B$ is independent of position because it is only a function of the volume fraction, which is independent of position). Once the strain rate is known, the flow rate can be calculated for a given height. The Bagnold constant can be evaluated from the constitutive relation

$$\mu\dot{\gamma} = A_B^2\dot{\gamma}^2. \qquad (3.27)$$

Using the energy conservation equation (3.3), this provides

$$A_B^2 = \left((\mu/T^{1/2})^{3/2}/R^{1/2}\right). \qquad (3.28)$$

Since both $(\mu/T^{1/2})$ and $R$ diverge proportional to $\phi^2\chi(\phi)$ in the limit $\phi \to \phi_c$, equation (3.28) indicates that $A_B \propto \phi_c\chi(\phi)^{1/2}$ near close packing,

$$A_B^2 \propto (\phi_c - \phi)^{-1}. \qquad (3.29)$$

Thus, equation (3.29) indicates that the Bagnold coefficient diverges proportional to $\chi^{1/2} \sim (\phi_c - \phi)^{-1/2}$ in the limit $\phi \to \phi_c$. From equation (3.25), $(\phi_c - \phi) \propto (\theta - \theta_0)$, and the Bagnold coefficient diverges proportional to $(\theta - \theta_0)^{-1/2}$.

The variation of the Bagnold coefficient with $\theta$ has been reported by Silbert *et al.* (2001) (their figure 18 actually shows the inverse of the Bagnold coefficient), and the Bagnold coefficient does diverge at $\theta_0$ in the three-dimensional simulations. In two-dimensional simulations, it appears that the static angle of repose is larger than $\theta_0$, and the Bagnold coefficient does not diverge at the static angle of repose. This makes it important to make a distinction between the static angle of repose, which is the angle at which flow is initiated as the angle of inclination is decreased, and the dynamic angle of friction $\theta_0$ obtained from the kinetic theory calculation, which is the minimum angle at which the shear production of energy is sufficient to sustain the flow as the angle of inclination is decreased.

The analysis of Louge (2003), was similar to that presented here, in identifying a region of steady flow in the centre and boundary layers at the top and bottom surfaces. Bocquet *et al.* (2002) used a slightly different hydrodynamic model from the present one, and it is useful to compare the two studies. The hydrodynamic model used by Bocquet *et al.* (2002) is similar to the Navier–Stokes model used here, where the stress tensor contains a pressure term and a viscous term given by Newton's law of viscosity. However, the coefficient of viscosity used in Bocquet *et al.* (2002) has a stronger divergence than the pair distribution function, and it diverges as $(1 - \phi/\phi_c)^{-\beta}$ near close packing, where the coefficient $\beta$ is greater than 1 (it was assumed to be 1.5 in Bocquet *et al.* 2002). This results in qualitatively different results for the following reason. In equation (3.2), the ratio of shear and normal stresses is proportional to $(\mu R)^{1/2}/p$ in the Navier–Stokes approximation, where $R$ is the rate of dissipation of energy. This ratio approaches a constant value if $\mu$, $R$ and $p$ diverge proportional to the pair distribution function, as expected in the kinetic theory for dense gases. However, if the viscosity diverges faster than the rate of dissipation and pressure as the close packing density is approached, this ratio diverges. This indicates that flow occurs near close packing only if $\tan(\theta) \to \infty$ or $\theta \to (\pi/2)$, and the density increases as the angle of inclination is decreased below $(\pi/2)$. This behaviour is illustrated in figure 2 for a modified viscosity $\mu_m$ defined in a manner slightly different from Bocquet *et al.* (2002), but which has the same behaviour in the high-density limit,

$$\mu_m = \mu\left(1 + \frac{\alpha^{0.5}}{(1 - \phi/\phi_c)^{0.5}}\right), \tag{3.30}$$

where $\alpha$ is a cutoff value for $(1 - \phi/\phi_c)$, which is assumed to be 0.005 in figure 2. It is apparent that equation (3.30) converges to the dense gas viscosity $\mu$ for $(1 - \phi/\phi_c) \gg \alpha$, while it has a divergence proportional to $(1 - \phi/\phi_c)^{-1.5}$ for $(1 - \phi/\phi_c) \ll \alpha$. The result of this viscosity modification on the flow curves is shown in figure 2, and it is observed that $\tan(\theta)$ is close to the value for smooth particles at low volume fraction, but diverges as the close packing volume fraction is approached in the adiabatic approximation.

Finally, we examine the minimal model that is required to provide realistic results for the flow down an inclined plane, and indicate how the coefficients in the model could be obtained independently from simulations for collisional models different from those discussed here. The simplest simulation requiredfor obtaining the coefficients

in the constitutive relations is the shear flow in the absence of gravity, using Lees–Edwards boundary conditions. Since there is no imposed time scale in the problem, it is convenient to express all variables in terms of the strain rate $\dot{\gamma}$. The shear viscosity $\mu$ in this case is the ratio of the shear stress and the strain rate. The dissipation coefficient $R$ can then be determined from the energy balance equation at steady state using the measured mean square velocity $T$ (note that $G_{ii}$ is zero for a steady shear flow). The isotropic part of the stress tensor, obtained from simulations, is $(-p + (\mathscr{B}_{SS} - \mathscr{B}_{AA})\dot{\gamma}^2/12)$, while the first and second normal stress differences are $\mathscr{A}_{SAS}\dot{\gamma}^2$ and $(cA_{SAS}/2 + (\mathscr{A}_{SS} - \mathscr{A}_{AA})/4)\dot{\gamma}^2$. Therefore, the measurement of all the components of the stress tensor can be used to provide the modified pressure $\bar{p} = (-p + (\mathscr{B}_{SS} - \mathscr{B}_{AA})\dot{\gamma}^2/12)$, as well as the coefficients $\mathscr{A}_{SAS}$ and $(\mathscr{A}_{SS} - \mathscr{A}_{AA})$. These coefficients could be determined as a function of the volume fraction, and then used to predict density as a function of angle of inclination in the flow. The coefficients $\mathscr{A}_{SS}$ and $\mathscr{A}_{AA}$ cannot be determined independently in a linear shear flow, but the coefficient $\mathscr{A}_{AA}$ could be determined for a rotating flow, for which the symmetric part of the rate of deformation tensor is identically zero. The Burnett correction with the modified pressure (which includes all the isotropic components), and the terms proportional to $\mathscr{A}_{SS}$, $\mathscr{A}_{AA}$ and $\mathscr{A}_{SAS}$ would constitute the minimal model required to capture accurately the dynamics of a flow with no radial component, such as the flow down an inclined plane. These coefficients could be used to determine the angle of inclination as a function of density. The Bagnold coefficient could then be calculated using equation (3.28), and this could be used to specify the strain rate as a function of the angle of inclination.

## 4. Conclusions

The constitutive relation for the stress tensor for the granular flow of rough particles was derived using a simple collision model for rough particles which contains a normal and tangential coefficient of restitution. A more realistic 'partially rough' particle model was also considered, in which frontal collisions are rough, whereas grazing collisions are smooth. A perturbation expansion of the Boltzmann equation can be employed only if the dissipation of energy in a collision is small compared to the energy of a particle. The small parameter in the expansion $\varepsilon$ is defined such that $\varepsilon^2$ is equal to $1 - e_n$, and $\varepsilon^2$ is proportional to the difference between $e_t$ and $\pm 1$. Though this model is not realistic, it is useful because it can be solved using an expansion in a small parameter, and it provides the qualitative form of the stress tensor expected for more realistic models.

An important length scale in the system is the 'conduction length' $(\lambda/(1 - e_n)^{1/2})$, where $\lambda$ is the mean free path. The analysis is restricted to the case where the length scale is large compared to the conduction length, so that the rate of conduction of energy is small compared to the rates of production (due to shear) and dissipation (due to inelastic collisions). It is appropriate to use the 'adiabatic approximation', where there is a local balance between the rates of production of energy due to shear and the collisional dissipation. A hydrodynamic description in this case incorporates only the mass and momenta, since energy is not a conserved variable.

In the granular flow of rough particles, the angular momentum is not conserved in a reference frame moving with the particles, and so the local angular velocity is expressed in terms of the local rate of deformation using the conservation equation for the particle angular velocity. The local angular velocity is equal to

half the vorticity in the leading approximation for rough particles, though there are higher-order contributions due to streaming terms in the Boltzmann equation. The principle of equipartition of energy is applicable in the rough particle limit, and the energy in the rotational modes is equal to that in the translational modes in the leading approximation. The pressure–density relationship for rough particles is identical to that of smooth particles. The shear viscosity for rough particles is higher by about 10 % in the dilute limit, and about 50 % in the dense limit than that for smooth particles. There is a significant difference in the bulk viscosity, however, and it is found that the bulk viscosity for rough particles is finite in the dilute limit, whereas the bulk viscosity for smooth particles is zero in this limit. This is due to the possibility of transport of energy between the translational and internal modes in the rough particle system. In the Burnett-order contributions to the stress tensor, it is found that there is an antisymmetric contribution to the stress tensor for the rough particles even when the local angular velocity is equal to half the vorticity, which is not present in the flow of smooth particles. It turns out that this contribution is identically zero for a linear shear flow, but could be non-zero for other types of flows. There are numerical differences in the other Burnett coefficients as well.

In the case of partially rough particles, it is found that the local angular velocity is equal to a quarter of the vorticity (which is half the angular velocity for rough particles) since exchange of angular velocity takes place in only half the collisions when the roughness angle is $(\pi/4)$. In addition, the average energy in the rotational modes is equal to half the energy in the translational modes in the leading approximation, indicating that the equipartition principle does not apply in this case even in the energy conserving limit where the coefficients of restitution approach $\pm 1$ and the strain rate approaches zero. The results of the partially rough particle model have important implications for micropolar theories of granular flows, in which constitutive relations are written for the stress and the 'couple stress'. In the constitutive relations, the stress contains an antisymmetric component proportional to the difference between the local angular velocity and half the local vorticity. In the absence of gradients in the angular velocity, these theories predict that the angular velocity is always equal to half the vorticity. The present 'partially rough' particle analysis indicates that for realistic collisions involving stick and slip, the angular velocity is not always equal to half the vorticity, but could be some other fraction of the vorticity depending on the collision model. Therefore, it would be necessary to modify the conventional micropolar theories if they are to be used for granular flows with realistic collision models.

The constitutive relations obtained here were applied to the granular flow down an inclined plane under gravity. Several qualitative features which are observed in simulations are predicted by the constitutive relations for rough and partially rough particles, if the Burnett terms are incorporated.

(*a*) The constant density in the bulk of the flow if the height is large compared to the conduction length, and the rate of conduction of energy is neglected in the energy equation.

(*b*) The minimum angle required for the onset of flow, and the maximum angle beyond which there is no steady flow. In the present analysis, the minimum angle is not determined by a dynamical friction condition, but by the energy balance requirement that it is necessary to generate sufficient energy by the mean shear to balance the rate of dissipation due to particle interactions.

(*c*) The analysis also shows that this minimum angle is remarkably insensitive to the values of the coefficients of restitution. However, this prediction should be treated with caution, since we are using a perturbation expansion about the limit of elastic collisions.

(*d*) The decrease in the volume fraction as the angle of inclination is increased.

(*e*) The small first normal stress difference, and its variation between positive and negative values for different collision models.

(*f*) The negative second normal stress difference which is much larger in magnitude than the first normal stress difference.

It should be noted that the above results are obtained only for the rough and partially rough models if the Burnett terms are included in the expression for the stress tensor. These are not obtained if the Burnett terms are not included, and they are not obtained for the smooth particle model even if the Burnett terms are included.

This suggests that the essential dynamics of the flow down an inclined plane is successfully captured by a kinetic theory approach, though it is necessary to include sufficient detail in the collision model and to incorporate at least the second-order term in the constitutive relation for the stress. In order to proceed further, it is necessary to make numerical comparisons of the stresses between theory and simulations for the same collision model. The simulation models used so far incorporate frictional collisions with a friction coefficient, which is difficult to handle analytically in kinetic theory. Therefore, it is necessary to incorporate simpler collision models in simulations, as well as to try and extend kinetic theory to frictional collisions. Another source of difficulty in numerical comparisons is the form of the pair distribution function. The pair distribution function in a shear flow is likely to be anisotropic in general, and different from the simple forms, such as the Carnahan–Starling form, presently used in kinetic theories. A systematic calculation of the pair distribution function is an additional input required for the numerical prediction of stresses using the kinetic theory approach.

This research was supported by the Swarnajayanthi Fellowship, Department of Science and Technology, Government of India.

## Appendix A. Comparison of Chapman–Enskog procedure and present procedure

The Chapman–Enskog procedure for determining the transport coefficients is as follows. At equilibrium, the velocity distribution function has the form

$$F(\boldsymbol{c}, \omega) = \frac{1}{(2\pi T)^3} \exp\left( - \frac{c_i^2}{2T} - \frac{\mathscr{I}\omega_i^2}{2T} \right), \tag{A 1}$$

where $T$ is the temperature. In a system close to equilibrium, it is assumed that the variation of the distribution function with position and time is due only to the spatial variation of the density, mean velocity and temperature. The perturbation to the distribution function is of the form

$$f(\boldsymbol{x}, \boldsymbol{c}, \omega) = F(c_i, \omega_i)\left[1 + \Phi_i^T \partial_i T + \Phi_{ij}^S \partial_i U_j + \Phi^B \partial_i U_i\right], \tag{A 2}$$

where $F(c_i, \omega_i)$ is the Maxwell–Boltzmann distribution, and the superscripts $T$, $S$ and $B$ indicate that the corresponding corrections to the equilibrium distribution give rise to the thermal conductivity, shear viscosity and bulk viscosity, respectively. The

transport rates are determined as a function of these coefficients,

$$\left.\begin{aligned}\lambda &= -\frac{1}{2}\int_{\boldsymbol{c},\omega} F(c_i,\omega_i)(c^2+\mathscr{I}\omega^2)c_i\Phi_i^T,\\ \mu &= \int_{\boldsymbol{c},\omega} F(c_i,\omega_i)\left(c_ic_j-(\delta_{ij}/3)c_k^2\right)\Phi_{ij}^S,\\ \mu_B &= \int_{\boldsymbol{c},\omega} F(c_i,\omega_i)c^2\Phi^B,\end{aligned}\right\} \tag{A 3}$$

where $\int_{\boldsymbol{c},\omega} \equiv \int \mathrm{d}\boldsymbol{c}\int \mathrm{d}\omega$. The leading-order distribution function, (A 1), is inserted into the left-hand side of the Boltzmann equation (2.1), to obtain

$$F\left[\left(\frac{c^2}{2T}-\frac{\mathscr{I}\omega^2}{2T}-1\right)\frac{c_i\partial_i T}{T}+\frac{c_ic_j\partial_iU_j}{T}+\left(\frac{c_i^2}{3}-\frac{\mathscr{I}\omega_i^2}{3}\right)\partial_kU_k\right]=\left.\frac{\partial_c f}{\partial t}\right|_1, \tag{A 4}$$

where $\star|_1$ is the first correction to $\star$. Equation (A 2) is inserted into the right-hand side of (A 4), and solved in order to obtain the $\Phi_i^T$ and $\Phi_{ij}^S$ and $\Phi^B$ in (A 2).

For a gas of smooth particles, $\boldsymbol{\Phi}_T$, $\boldsymbol{\Phi}_S$ and $\boldsymbol{\Phi}_B$ can be expressed in terms of the fluctuating velocities as

$$\left.\begin{aligned}\Phi_i^T &= \phi^T(c)c_i\left(\frac{c^2}{2T}-\frac{5}{2}\right),\\ \Phi_{ij}^S &= \phi^S(c)(c_ic_j-(\delta_{ij}/3)c^2),\\ \Phi^B &= \phi^B(c)\left(\frac{c^2}{2T}-\frac{3}{2}\right),\end{aligned}\right\} \tag{A 5}$$

where $\phi^T$, $\phi^S$ and $\phi^B$ are scalar functions of the velocity fluctuations. The above forms for $\Phi_i^T$, $\Phi_{ij}^S$ and $\Phi_B$ are deduced from their respective tensor order, as well as from the requirement that the perturbation to the distribution function has to be orthogonal to the homogeneous solution for the existence of a solution for the inhomogeneous equation (A 4). The solution for $\phi^T$ is obtained by multiplying the Boltzmann equation by $c_i$ and integrating over the particle velocities. An expansion in Sonine polynomials is used for $\phi^T$. However, it is found that the results are numerically accurate to within 1.2 % if only the leading term in the Sonine polynomial expansion is retained, which is equivalent to considering $\phi^T$ to be a constant. Similarly, $\Phi^S$ is obtained by multiplying the Boltzmann equation by $(c_ic_j-(\delta_{ij}/3)c^2)$, and integrating over all particle velocities. In this case also, the results are numerically accurate to within 1.2 % if $\phi^S$ is considered to be a constant. The thermal conductivity and the viscosity are then obtained from the known values of $\phi^T$ and $\phi^S$. The constant $\phi^B$ is found to be identically zero in the dilute limit.

For a gas of rough particles, the most general expressions for $\boldsymbol{\Phi}_T$ and $\boldsymbol{\Phi}_U$ also include dependences on the angular velocities of the particles,

$$\left.\begin{aligned}\Phi_i^T &= \phi^T(c,\omega)c_i\left[\left(\frac{c^2}{2T}-\frac{5}{2}\right)+\left(\frac{\mathscr{I}\omega^2}{2T}-\frac{3}{2}\right)\right],\\ \Phi_{ij}^S &= \phi^{S1}(c,\omega)(c_ic_j-(\delta_{ij}/3)c^2)+\phi^{S2}(c,\omega)(\omega_i\omega_j-(\delta_{ij}/3)\omega^2),\\ \Phi^B &= \phi^B(c,\omega)\left[\left(\frac{c^2}{2T}-\frac{3}{2}\right)-\left(\frac{\mathscr{I}\omega^2}{2T}-\frac{3}{2}\right)\right].\end{aligned}\right\} \tag{A 6}$$

These forms of the perturbations are inserted into the Boltzmann equation, and the equation is solved to obtain the functions $\phi^T$, $\phi^{S1}$, $\phi^{S2}$ and $\phi^B$, which are functions

of the magnitudes of the fluctuating velocities and angular velocities. A Sonine polynomial expansion is used for these functions, but numerically accurate results are obtained if only the first term in the series is retained. The transport properties are then obtained using equations (A 3).

The conductivity obtained using the Chapman–Enskog procedure in the dilute limit is given by

$$\lambda = \frac{9}{16}\sqrt{\frac{T}{\pi}}\frac{(1+4\mathscr{I})^2(37+604\mathscr{I}+50\mathscr{I}^2)}{12+300\mathscr{I}+404\mathscr{I}^2+816\mathscr{I}^2}. \tag{A 7}$$

The bulk viscosity obtained using the Chapman–Enskog procedure,

$$\mu_B = \frac{1}{128}\sqrt{\frac{T}{\pi}}\frac{(1+4\mathscr{I})^2}{\mathscr{I}} \tag{A 8}$$

is identical to that obtained by the present moment expansion procedure (equation (2.59)). This is because the procedure used here, which is to multiply the Boltzmann equation by $(c_i^2/2-\mathscr{I}\omega_i^2/2)$ and integrate over velocity space, is equivalent to inserting the correction proportional to $\Phi^B$ in equation (A 2), and averaging over all velocities (assuming that $\phi^B$ in equation (A 6) is a constant). However, the term proportional to $\phi_{S2}$ in the equation for $\boldsymbol{\Phi}_S$, is neglected in the expansion of Pidduck (1922), and the resultant expression for the viscosity is

$$\mu = \frac{15}{16}\sqrt{\frac{T}{\pi}}\frac{(1+4\mathscr{I})^2}{3+26\mathscr{I}}. \tag{A 9}$$

In the present analysis, the terms proportional to $\phi^{S1}$ and $\phi^{S2}$ are retained in the expansion in (A 6), and so the viscosity obtained (equation (2.59)) is higher than that for gases of smooth particles by about 10 %, whereas the Pidduck expression (A 9) is higher than that for gases of smooth particles by only 5 %.

## Appendix B. Velocity and angular velocity change in a collision between rough particles

Consider a collision between two particles with positions $\boldsymbol{x}$ and $\boldsymbol{x}^*$, with velocities and angular velocities $(\boldsymbol{u},\omega)$ and $(\boldsymbol{u}^*,\omega^*)$, such that the unit vector from the particle at $\boldsymbol{x}$ to the particle at position $\boldsymbol{x}^*$ is $\boldsymbol{k}$. The position of the contact is then $\boldsymbol{x}_c=\boldsymbol{x}+\boldsymbol{k}/2=\boldsymbol{x}^*-\boldsymbol{k}/2$ (note that we are non-dimensionalizing all lengths by the diameter of a particle, so that the distance from the centre to a position on the surface is just 1/2 in dimensionless units.) The relative velocity at the point of contact is

$$\begin{aligned}\boldsymbol{g} &= \boldsymbol{u}-\boldsymbol{u}^*-\big((\boldsymbol{x}_c-\boldsymbol{x})\times\omega-(\boldsymbol{x}_c-\boldsymbol{x}^*)\times\omega^*\big)\\ &= \boldsymbol{u}-\boldsymbol{u}^*-\tfrac{1}{2}\boldsymbol{k}\times(\omega+\omega^*).\end{aligned} \tag{B 1}$$

Here, we use the convention that for a rigid body rotating with angular velocity $\boldsymbol{\omega}$, the linear velocity $\boldsymbol{u}$ at a point located at a vector distance $\boldsymbol{r}$ from the centre of rotation is $\boldsymbol{u}=\omega\times\boldsymbol{r}$. In indicial notation, equation (B 1) is written as

$$g_i = u_i-u_i^*-(\epsilon_{ijl}/2)k_j(\omega_l+\omega_l^*). \tag{B 2}$$

The components of the relative velocity parallel and perpendicular to the line joining centres at the point of contact before collision are,

$$\left.\begin{aligned} g_ik_i &= (u_i-u_i^*)k_i,\\ (\delta_{ij}-k_ik_j)g_j &= (\delta_{ij}-k_ik_j)(u_j-u_j^*)-(\epsilon_{ijl}k_j/2)(\omega_l+\omega_l^*).\end{aligned}\right\} \tag{B 3}$$

The post-collisional relative velocity at the point of contact, $g_i'$, is related in an identical manner to the post-collisional linear and angular velocities, $(u_i', \omega_i')$ and $(u_i^{*\prime}, \omega_i^{*\prime})$. In the collision model employed here, the post-collisional relative velocity in the direction of the line joining is $-e_n$ times its pre-collisional value, while the post-collisional relative velocity in the direction perpendicular to the line joining the centres is $-e_t$ times its pre-collisional value.

$$\left.\begin{aligned} g_i' k_i &= -e_n g_i k_i, \\ (\delta_{ij} - k_i k_j) g_j' &= -e_t (\delta_{ij} - k_i k_j) g_j. \end{aligned}\right\} \tag{B 4}$$

If $J_i$ is the impulse exerted on the particle at $\boldsymbol{x}$ by the particle at $\boldsymbol{x}^*$ in a collision, the linear and angular velocities of the particles before and after collision are,

$$\left.\begin{aligned} u_i' &= u_i + J_i, \quad u_i^{*\prime} = u_i^* - J_i, \\ \omega_i' &= \omega_i + (\epsilon_{ijk}/2\mathscr{I}) k_j J_k, \quad \omega_i^{*\prime} = \omega_i^* + (\epsilon_{ijk}/2\mathscr{I}) k_j J_k, \end{aligned}\right\} \tag{B 5}$$

where $\mathscr{I}$ is the moment of inertia scaled by the particle mass and the square of the diameter. (Note that the particle mass has been set equal to 1 while calculating the impulse.) In calculating the angular velocity difference, we have used the convention that if a force $\boldsymbol{F}$ is exerted at a position with displacement $\boldsymbol{r}$ from the centre of a rigid body, then the torque $\boldsymbol{L}$ is given by $\boldsymbol{L} = \boldsymbol{r} \times \boldsymbol{F}$. Using the above expressions, we can write the impulse in terms of the relative velocities at the point of contact,

$$\left.\begin{aligned} k_i (g_i' - g_i) &= 2 J_i k_i, \\ (\delta_{ij} - k_i k_j)(g_j' - g_j) &= 2(\delta_{ij} - k_i k_j) J_j ((1 + 4\mathscr{I})/4\mathscr{I}). \end{aligned}\right\} \tag{B 6}$$

Using equation (B 4) for the pre- and post-collisional velocities of surface at the point of contact, the impulse $J_i$ in equation (B 6) can be expressed in terms of the pre-collisional linear and angular velocities,

$$\left.\begin{aligned} J_i k_i &= -((1 + e_n)/2)(u_i - u_i^*) k_i, \\ (\delta_{ij} - k_i k_j) J_j &= -((1 + e_t)/2)(4\mathscr{I}/(1 + 4\mathscr{I}))((\delta_{ij} - k_i k_j)(u_j - u_j^*) \\ &\quad -(\epsilon_{ijl}/2) k_j (\omega_l + \omega_l^*)). \end{aligned}\right\} \tag{B 7}$$

Using equation (B 7) for the impulse and equation (B 5) for the relations between the pre- and post-collisional velocities, we find,

$$\left.\begin{aligned} u_i' - u_i &= -((1 + e_n)/2)(u_j - u_j^*) k_j k_i - ((1 + e_t)/2)(4\mathscr{I}/(1 + 4\mathscr{I})) \\ &\quad \times ((\delta_{ij} - k_i k_j)(u_j - u_j^*) - (\epsilon_{ijl}/2) k_j (\omega_l + \omega_l^*)), \\ \omega_i' - \omega_i &= -((1 + e_t)/2)(4\mathscr{I}/(1 + 4\mathscr{I}))(1/2\mathscr{I})(\epsilon_{ijl} k_j (u_l - u_l^*) \\ &\quad + (1/2)(\delta_{ij} - k_i k_j)(\omega_j + \omega_j^*)). \end{aligned}\right\} \tag{B 8}$$

## Appendix C. Calculation of substantial derivatives

The convective terms in the first correction to the second moment equations (2.51) and (2.52) are calculated as follows. The left-hand side of equation (2.51) is given by

$$\left.\begin{aligned}
&\rho\frac{\mathrm{D}T_{ij}^{(1)}}{\mathrm{D}t}+\rho\big(T_{ik}^{(1)}G_{kj}+T_{jk}^{(1)}G_{ki}\big)\\
&=\rho\frac{\mathrm{D}\big(-Q_TT^{1/2}S_{ij}-(\delta_{ij}/3)Q_{TI}T^{1/2}G_{kk}\big)}{\mathrm{D}t}+\rho\big(-T^{1/2}Q_T(S_{ik}G_{kj}+S_{jk}G_{ki})\\
&\quad-T^{1/2}Q_{TI}(G_{kk}/3)(G_{ij}+G_{ji})\big),\\
&=\rho\frac{\mathrm{D}(-Q_TT^{1/2}S_{ij})}{\mathrm{D}t}-\frac{\rho\delta_{ij}}{3}\frac{\mathrm{D}\big(Q_{TI}T^{1/2}G_{kk}\big)}{\mathrm{D}t}\\
&\quad-\rho T^{1/2}Q_T(2S_{ik}S_{kj}+S_{ik}A_{kj}+S_{jk}A_{ki}+(2/3)S_{ij}G_{ll})\\
&\quad-\rho T^{1/2}Q_{TI}\big((2S_{ij}G_{kk}/3)+\big(2\delta_{ij}G_{kk}^2/9\big)\big).
\end{aligned}\right\}\tag{C 1}$$

The first two terms on the left-hand side of equation (C 1) can be simplified as follows.

$$\begin{aligned}
\rho\frac{\mathrm{D}\big(Q_TT^{1/2}S_{ij}\big)}{\mathrm{D}t}&=\rho\left(Q_TT^{1/2}\frac{\mathrm{D}S_{ij}}{\mathrm{D}t}+S_{ij}T^{1/2}\frac{\mathrm{d}Q_T}{\mathrm{d}\rho}\frac{\mathrm{D}\rho}{\mathrm{D}t}+\frac{Q_TS_{ij}}{2T^{1/2}}\frac{\mathrm{D}T}{\mathrm{D}t}\right)\\
&=\rho\left(Q_TT^{1/2}\frac{\mathrm{D}S_{ij}}{\mathrm{D}t}-S_{ij}T^{1/2}\rho G_{kk}\frac{\mathrm{d}Q_T}{\mathrm{d}\rho}-\frac{Q_TS_{ij}}{2T^{1/2}}\frac{pG_{kk}}{\rho C_v}\right)\\
&=\rho\left(Q_TT^{1/2}\frac{\mathrm{D}S_{ij}}{\mathrm{D}t}-S_{ij}T^{1/2}\rho G_{kk}\frac{\mathrm{d}Q_T}{\mathrm{d}\rho}-\frac{Q_TS_{ij}T^{1/2}(1+4\phi\chi)G_{kk}}{C_v}\right),
\end{aligned}\tag{C 2}$$

and

$$\begin{aligned}
\rho\frac{\mathrm{D}(Q_{TI}T^{1/2}G_{kk})}{\mathrm{D}t}&=\rho\left(Q_{TI}T^{1/2}\frac{\mathrm{D}G_{kk}}{\mathrm{D}t}+G_{kk}T^{1/2}\frac{\mathrm{d}Q_{TI}}{\mathrm{d}\rho}\frac{\mathrm{D}\rho}{\mathrm{D}t}+\frac{Q_TG_{kk}}{2T^{1/2}}\frac{\mathrm{D}T}{\mathrm{D}t}\right)\\
&=\rho\left(Q_{TI}T^{1/2}\frac{\mathrm{D}G_{kk}}{\mathrm{D}t}-G_{kk}^2T^{1/2}\rho\frac{\mathrm{d}Q_{TI}}{\mathrm{d}\rho}-\frac{Q_{TI}G_{kk}}{2T^{1/2}}\frac{pG_{kk}}{\rho C_v}\right)\\
&=\rho\left(Q_{TI}T^{1/2}\frac{\mathrm{D}G_{kk}}{\mathrm{D}t}-G_{kk}^2T^{1/2}\rho\frac{\mathrm{d}Q_{TI}}{\mathrm{d}\rho}-\frac{Q_{TI}G_{kk}^2T^{1/2}(1+4\phi\chi)}{C_v}\right)
\end{aligned}\tag{C 3}$$

where the mass conservation equation $(D\rho/Dt)=\rho G_{kk}$ and the leading order energy conservation equation $(DT/Dt)=-(pG_{kk}/\rho C_v)$ have been used to simplify the right sides of equations (C 2) and (C 3). The substantial derivative of the symmetric traceless and isotropic parts of the rate of deformation tensor is simplified as

$$\begin{aligned}
\frac{\mathrm{D}S_{ij}}{\mathrm{D}t}&=\frac{1}{2}\left(\frac{\partial}{\partial t}+u_l\frac{\partial}{\partial x_l}\right)\left(\frac{\partial u_i}{\partial x_j}+\frac{\partial u_j}{\partial x_i}-\frac{2\delta_{ij}}{3}\frac{\partial u_k}{\partial x_k}\right)\\
&=\frac{1}{2}\left(\frac{\partial}{\partial x_j}\frac{\mathrm{D}u_i}{\mathrm{D}t}-G_{ik}G_{kj}+\frac{\partial}{\partial x_i}\frac{\mathrm{D}u_j}{\mathrm{D}t}-G_{jk}G_{ki}-\frac{2\delta_{ij}}{3}\frac{\partial}{\partial x_k}\frac{\mathrm{D}u_k}{\mathrm{D}t}+\frac{2\delta_{ij}}{3}G_{kl}G_{lk}\right)\\
&=\frac{1}{2}\left(\frac{\partial}{\partial x_j}\left(\frac{1}{\rho}\frac{\partial\sigma_{ik}}{\partial x_k}\right)+\frac{\partial}{\partial x_i}\left(\frac{1}{\rho}\frac{\partial\sigma_{jk}}{\partial x_k}\right)-\frac{2\delta_{ij}}{3}\frac{\partial}{\partial x_k}\left(\frac{1}{\rho}\frac{\partial\sigma_{kl}}{\partial x_l}\right)\right)\\
&\quad-S_{ik}S_{kj}-A_{ik}A_{kj}-\frac{2S_{ij}G_{kk}}{3}+\frac{\delta_{ij}(S_{kl}S_{lk}+A_{kl}A_{lk})}{3}
\end{aligned}\tag{C 4}$$

$$\begin{aligned}\frac{\mathrm{D}G_{kk}}{\mathrm{D}t} &= \left(\frac{\partial}{\partial t}+u_l\frac{\partial}{\partial x_l}\right)\left(\frac{\partial u_k}{\partial x_k}\right)\\ &= \frac{\partial}{\partial x_k}\frac{\mathrm{D}u_k}{\mathrm{D}t}-G_{kl}G_{lk}\\ &= \frac{\partial}{\partial x_k}\left(\frac{\partial \sigma_{kl}}{\partial x_l}\right)-S_{kl}S_{lk}-A_{kl}A_{lk}-\frac{G_{kk}^2}{3}\end{aligned} \tag{C 5}$$

where $\sigma_{ij}$ is the stress tensor, and the momentum conservation equation $(Du_i/Dt)=\rho^{-1}(\partial\sigma_{ij}/\partial x_j)$ has been used to simplify the right sides of equations (C 4) and (C 5). Adding these contributions, we get

$$\begin{aligned}&\rho\frac{\mathrm{D}T_{ij}^{(1)}}{\mathrm{D}t}+\rho\left(T_{ik}^{(1)}G_{kj}+T_{jk}^{(1)}G_{ki}\right)\\ &=\rho Q_T T^{1/2}\left(S_{ij}G_{kk}\left(\frac{\rho}{Q_T}\frac{\mathrm{d}Q_T}{\mathrm{d}\rho}+\frac{1+4\phi\chi}{C_v}\right)\right.\\ &\quad-\frac{\rho Q_T T^{1/2}}{2}\left(\frac{\partial}{\partial x_j}\left(\frac{1}{\rho}\frac{\partial\sigma_{ik}}{\partial x_k}\right)+\frac{\partial}{\partial x_i}\left(\frac{1}{\rho}\frac{\partial\sigma_{jk}}{\partial x_k}\right)-\frac{2\delta_{ij}}{3}\frac{\partial}{\partial x_k}\left(\frac{1}{\rho}\frac{\partial\sigma_{kl}}{\partial x_l}\right)\right)\Big)\\ &\quad-\rho Q_T T^{1/2}\left(S_{ik}S_{kj}+\frac{\delta_{ij}}{3}S_{kl}S_{lk}+S_{ik}A_{kj}+S_{jk}A_{ki}-A_{ik}A_{kj}+\frac{\delta_{ij}}{3}A_{kl}A_{lk}\right)\\ &\quad+\frac{\rho Q_{TI}T^{1/2}\delta_{ij}}{3}\left(G_{kk}^2\left(\frac{\rho}{Q_{TI}}\frac{\mathrm{d}Q_{TI}}{\mathrm{d}\rho}+\frac{1+4\phi\chi}{C_v}\right)\right.\\ &\quad\left.-\frac{\partial}{\partial x_k}\left(\frac{1}{\rho}\frac{\partial\sigma_{kl}}{\partial x_l}\right)+S_{kl}S_{lk}+A_{kl}A_{lk}-\frac{G_{kk}^2}{3}\right)-\frac{2\rho T^{1/2}Q_{TI}S_{ij}G_{kk}}{3}\end{aligned} \tag{C 6}$$

A similar procedure is used for simplifying the left side of equation (2.52).

$$\begin{aligned}\rho\frac{\mathrm{D}\Upsilon_{ij}^{(1)}}{\mathrm{D}t}&=\rho Q_\Upsilon T^{1/2}\left(S_{ij}G_{kk}\left(\frac{\rho}{Q_\Upsilon}\frac{\mathrm{d}Q_\Upsilon}{\mathrm{d}\rho}+\frac{1+4\phi\chi}{C_v}\right)\right.\\ &\quad-\frac{\rho Q_\Upsilon T^{1/2}}{2}\left(\frac{\partial}{\partial x_j}\left(\frac{1}{\rho}\frac{\partial\sigma_{ik}}{\partial x_k}\right)+\frac{\partial}{\partial x_i}\left(\frac{1}{\rho}\frac{\partial\sigma_{jk}}{\partial x_k}\right)-\frac{2\delta_{ij}}{3}\frac{\partial}{\partial x_k}\left(\frac{1}{\rho}\frac{\partial\sigma_{kl}}{\partial x_l}\right)\right)\Big)\\ &\quad+\rho Q_\Upsilon T^{1/2}\left(S_{ik}S_{kj}-\frac{\delta_{ij}}{3}S_{kl}S_{lk}+A_{ik}A_{kj}-\frac{\delta_{ij}}{3}A_{kl}A_{lk}\right)\\ &\quad+\frac{\rho Q_{\Upsilon I}T^{1/2}\delta_{ij}}{3}\left(G_{kk}^2\left(\frac{\rho}{Q_{TI}}\frac{\mathrm{d}Q_{TI}}{\mathrm{d}\rho}+\frac{1+4\phi\chi}{C_v}\right)\right.\\ &\quad\left.-\frac{\partial}{\partial x_k}\left(\frac{1}{\rho}\frac{\partial\sigma_{kl}}{\partial x_l}\right)+S_{kl}S_{lk}+A_{kl}A_{lk}+\frac{G_{kk}^2}{3}\right).\end{aligned} \tag{C 7}$$

Similarly, the substantial derivative of the leading contribution to the mean vorticity field (equation (2.31)) can be simplified as

$$\begin{aligned}\frac{\mathrm{D}\Omega_i^{(0)}}{\mathrm{D}t}&=(\partial_t+u_l\partial_l)\Omega_i^{(0)}\\ &=-\frac{\epsilon_{ijk}}{2}(\partial_t+u_l\partial_l)A_{jk}\\ &=-\frac{\epsilon_{ijk}}{2}(\partial_t+u_l\partial_l)(\partial_k u_j-\partial_j u_k)\\ &=-\frac{\epsilon_{ijk}}{2}(\partial_k((\partial_t+u_l\partial_l)u_j)-\partial_j((\partial_t+u_l\partial_l)u_k)-(\partial_k u_l)(\partial_l u_j)+(\partial_j u_l)(\partial_l u_k))\\ &=-\frac{\epsilon_{ijk}}{2}\left(\partial_k\left(\frac{\partial_l\sigma_{jl}}{\rho}\right)-\partial_j\left(\frac{\partial_l\sigma_{kl}}{\rho}\right)\right)+\epsilon_{ijk}(A_{jl}S_{lk}+S_{jl}A_{lk}).\end{aligned} \tag{C 8}$$

## REFERENCES


Bocquet, L., Errami, J. & Lubensky, T. C. 2002 Hydrodynamic model for a dynamical jammed-to-flowing transition in gravity driven granular media. *Phys. Rev. Lett.* **89**, 184 301–184 304.

Campbell, C. S. 1989 The stress tensor for simple shear flows of a granular material. *J. Fluid Mech.* **203**, 449–473.

Chapman, S. & Cowling, T. G. 1970 *The Mathematical Theory of Non-Uniform Gases.* Cambridge University Press.

Chou, C.-S. & Richman, M. W. 1998 Constitutive theory for homogeneous granular shear flows of highly inelastic spheres. *Physica* A **259**, 430–448.

Ernst, M. H., Cichocki, B., Dorfman, J. R., Sharma, J. & Van Beijeren, H. 1978 Kinetic theory of nonlinear viscous flow in two and three dimensions. *J. Stat. Phys.* **18**, 237–270.

Goldhirsch, I. 2003 Rapid granular flows, *Annu. Rev. Fluid Mech.* **35**, 267–293.

Herbst, O., Huthmann, M. & Zippelius, A. 2000 Dynamics of inelastically colliding spheres with Coulomb friction: relaxation of translational and rotational energy. *Gran. Matt.* **2**, 211–219.

Jenkins, J. T. & Richman, M. W. 1985 Grad's 13-moment system for a dense gas of inelastic spheres. *Arch. Rat. Mech. Anal.* **87**, 355–377.

Jenkins, J. T. & Savage, S. B. 1983 A theory for the rapid flow of identical, smooth, nearly elastic particles. *J. Fluid Mech.* **130**, 186–202.

Jenkins, J. T. & Zhang, C. 2002 Kinetic theory for identical, frictional, nearly elastic spheres. *Phys. Fluids* **14**, 1228–1235.

Kumaran, V. 2004 Constitutive relations and linear stability of a sheared granular flow. *J. Fluid Mech.* **506**, 1–43.

Louge, M.-Y. 2003 Model for dense granular flows down bumpy surfaces. *Phys. Rev.* E **67**, 061303–061313.

Louge, M.-Y. & Keast, S. C. 2001 On dense granular flows down flat frictional inclines. *Phys. Fluids* **13**, 1213–1233.

Lun, C. K. K. 1991 Granular flow of dense spheres. *J. Fluid Mech.* **233**, 539–559.

Lun, C. K. K. & Savage, S. B. 1987 A simple kinetic theory for granular flow of rough, inelastic, spherical particles. *Trans. ASME* E: *J. Appl. Mech.* **54**, 47–53.

Lun, C. K. K., Savage, S. B., Jeffrey, D. J. & Chepurniy, N. 1984 Kinetic theories for granular flow: inelastic particles in Couette flow and slightly inelastic particles in a general flow field. *J. Fluid Mech.* **140**, 223–256.

McCoy, B., Sandler, S. I. & Dahler, J. S. 1966 Transport theory of polyatomic fluids IV. The kinetic theory of a dense gas of perfectly rough spheres. *J. Chem. Phys.* 3485–3512.

Mitarai, N., Hayakawa, H. & Nakanishi, H. 2002 Collisional granular flow as a micropolar fluid. *Phys. Rev. Lett.* **88**, 174301.

Mohan, L. S., Rao, K. K. & Nott, P. R. 2002 A frictional Cosserat model for the slow shearing of granular materials. *J. Fluid Mech.* **457**, 377–409.

Pidduck, F. B. 1922 The kinetic theory of a special type of rigid molecule. *Proc. R. Soc. Lond.* A **101**, 101–112.

Pouliquen, O. 1999 Scaling laws in granular flows down rough inclined planes. *Phys. Fluids* **11**, 542–548.

Pouliquen, O. & Chevoir, F. 2002 Dense flows of dry granular material. *C. R. Phys.* **3**, 163–175.

Resibois, P. & de Leener, M. 1977 *Classical Kinetic Theory of Fluids.* Wiley.

Savage, S. B. & Jeffrey, D. J. 1981 The stress tensor in a granular flow at high shear rates. *J. Fluid Mech.* **110**, 255–272.

Sela, N. & Goldhirsch, I. 1998 Hydrodynamic equations for rapid flows of smooth inelastic spheres, to Burnett order. *J. Fluid Mech.* **361**, 41–74.

Sela, N., Goldhirsch, I. & Noskowicz, S. H. 1996 Kinetic theoretical study of a simply sheared two dimensional granular gas to Burnett order. *Phys. Fluids* **8**, 2337.

Silbert, L. E., Ertas, D., Grest, G. S., Halsey, T. C., Levine, D. & Plimpton, S. J. 2001 Granular flow down an inclined plane: Bagnold scaling and rheology. *Phys. Rev.* E **64**, 51302.

Theodosopulu, M. & Dahler, J. S. 1974*a* Kinetic theory of polyatomic liquids. I. The generalised moment method. *J. Chem. Phys.* **9**, 3567–3582.

Theodosopulu, M. & Dahler, J. S. 1974*b* Kinetic theory of polyatomic liquids. I. The rough sphere, rigid ellipsoid and square-well ellipsoid models. *J. Chem. Phys.* **9**, 4048–4057.

Walton, O. R. & Braun, R. L. 1986 Stress calculations for assemblies of inelastic spheres in uniform shear. *Acta Mech.* **63**, 74–86.